

# **Pullout Resistance of MSE Wall Steel Strip Reinforcement in Uniform Aggregate**

By

Mehari T. Weldu

Submitted to the graduate degree program in the Department of Civil, Environmental,  
and Architectural Engineering and the Graduate Faculty of the University of Kansas in  
partial fulfillment of the requirements for the degree of Master of Science.

.....

Chairperson, Dr. Jie Han

.....

Dr. Masoud K. Darabi

.....

Dr. Robert L. Parsons

Date Defended: 11/24/2015

The Thesis Committee for Mehari T. Weldu certifies that this is approved version of the following thesis:

**Pullout Resistance of MSE Wall Steel Strip  
Reinforcement in Uniform Aggregate**

.....  
**Dr. Jie Han, Chairperson**

Date Approved: 12/04/2015

## Abstract

A wide range of reinforcement-backfill combinations have been used in mechanically stabilized earth (MSE) walls. Steel strips are one type of reinforcement used to stabilize aggregate backfill through anchorage. In the current MSE wall design, pullout capacity of steel strips is evaluated to ensure internal stability of the reinforced mass. The pullout resistance of reinforcement is expressed in terms of a pullout resistance factor that measures the reinforcement-backfill interaction. This pullout resistance factor is commonly determined by performing pullout tests.

AASHTO (2012) LRFD Bridge Design and Specifications provides default values of the pullout resistance factor,  $F^*$ , for strip reinforcement embedded in backfill material with a uniformity coefficient of  $C_u \geq 4$ , where the uniformity coefficient is defined as the ratio of the particle size at 60% finer to that at 10% finer. However, for backfill with a uniformity coefficient,  $C_u < 4$ , AASHTO (2012) requires project-specific pullout tests. This AASHTO requirement has disqualified a large amount of aggregates produced in Kansas quarries or made them difficult and/or costly to be used in MSE wall construction. To address this problem, an experimental study was undertaken in the Geotechnical Engineering Laboratory at the University of Kansas to examine the effect of aggregate uniformity on pullout resistance of steel strips when the uniformity coefficient of aggregate,  $C_u < 4$ .

Twenty-two pullout tests were carried out on ribbed steel strip reinforcements embedded in six aggregate backfills of uniformity coefficients ranging from 1.4 to 14. The pullout resistance of each reinforcement-backfill combination was investigated under

normal stresses of 25, 41 and 69 kPa to simulate reinforcements placed at different depths of fill. Additionally, aggregate backfills with  $C_u=1.4$  and 14 were tested under normal stresses of 103 and 138 kPa to further evaluate the pullout resistance at higher depths. Each test sample was prepared in a consistent way to minimize variations. One of the important influence factor was degree of compaction.

The test results demonstrated that the overall trend for all types of aggregates was similar. The uniform aggregates generally behaved in the same way as the well-graded aggregates in terms of pullout resistance. The effect of aggregate uniformity was more obvious in the tests under a lower normal stress than under a higher normal stress. When the normal stress was at 69 kPa, there was no obvious effect of aggregate uniformity.

Furthermore, the pullout resistance factors obtained from this study were compared with the default  $F^*$  values for ribbed strip reinforcement provided by AASHTO (2012). The comparison shows that the pullout resistance factor for ribbed steel strips decreased with depth in the same way as suggested by AASHTO (2012). However, the  $F^*$  values recommended by AASHTO (2012) are conservative as compared with the test results when aggregate backfills with the uniformity coefficients ranging from 1.4 to 14 were used. In other words, the  $F^*$  values recommended by AASHTO (2012) can be used to design MSE walls with ribbed steel strips in aggregate backfills of the uniformity coefficient as low as 1.4 provided the backfill meets the AASHTO (2010) requirements.

**Dedication:**

**To my parents, Mr. Tesfagabr Weldu and Mrs. Nigisti Temesgen**

## **Acknowledgements**

First and foremost, I would like to express my sincere gratitude to my advisor, Prof. Jie Han, for giving me the opportunity to pursue my study under his mentorship and guidance. His guidance and professional advice will be my tools in my future career time. I would also like to thank Prof. Robert L. Parsons and Prof. Masoud K. Darabi for their valuable comments and serving as members of my examining committee.

This research project was financially sponsored by the Kansas Department of Transportation (KDOT) through the Kansas Transportation Research and New-Developments Program (KTRAN) program. Mr. James J. Brennan, the Chief Geotechnical Engineer of KDOT, was the monitor for this project. Bonner Spring Quarry APAC-Kansas City, Inc., provided the aggregate materials used in this study and Mr. Kyle E. Harbour, Quality Control Manager, with his staffs provided great assistance in the selection and collection of aggregate materials. The steel strips were provided by the Reinforced Earth Company.

The laboratory manager and technicians, Matthew Maksimowicz, David Woody, and Erick Nicholson, in Department of Civil, Environmental, and Architectural Engineering (CEAE) at the University of Kansas (KU) provided their technical support during the fabrication of the new pullout box and laboratory pullout testing. Last but not least, I would also like to express my appreciation to graduate students, S. Mustapha Rahmaninezhad, Jamal Kakrasul, Ghaith Abdulrasool, Jun Guo, Yan Jiang, and Fei Wang, from the Kansas University Geotechnical Society (KUGS) for their assistance in collecting aggregate materials from the quarry and performing laboratory experiment.

## Table of Contents

<b>Abstract.....</b>	<b>ii</b>
<b>Acknowledgements .....</b>	<b>vi</b>
<b>Table of Contents .....</b>	<b>vii</b>
<b>List of Tables .....</b>	<b>ix</b>
<b>List of Figures.....</b>	<b>x</b>
<b>CHAPTER 1 INTRODUCTION .....</b>	<b>1</b>
1.1. Background .....	1
1.2. Research Problem Statement.....	4
1.3. Research Objective.....	5
1.4. Research Approach .....	6
1.5. Thesis Organization.....	6
<b>CHAPTER 2 LITERATURE REVIEW .....</b>	<b>8</b>
2.1 Stress Transfer Mechanism .....	8
2.2 Guidelines for Pullout Resistance Determination .....	11
2.3 Past Pullout Tests .....	14
2.3.1 Laboratory Pullout Tests.....	14
2.3.2 Field Pullout Tests .....	18
<b>CHAPTER 3 TEST MATERIALS AND APPARATUS.....</b>	<b>19</b>
3.1 Backfill Material .....	19
3.2 Reinforcement .....	21
3.3 Pullout Test Apparatus .....	22
<b>CHAPTER 4 TEST PROCEDURE AND DATA ACQUISITION .....</b>	<b>25</b>
4.1 Pullout Test Procedure .....	25
4.1.1 Test Sample Preparation .....	25
4.1.2 Application of Normal Stress.....	27
4.1.3 Application of Pullout Load.....	28

4.2 Data Acquisition.....	29
<b>CHAPTER 5 TEST RESULTS AND DATA ANALYSIS .....</b>	<b>31</b>
5.1 Triaxial Test Results.....	31
5.2 Pullout Test Results.....	33
5.3 Pullout Force and Displacement .....	33
5.4 Pullout Resistance Factor, $F^*$ .....	39
<b>CHAPTER 6 CONCLUSIONS AND RECOMMENDATIONS .....</b>	<b>43</b>
6.1 Conclusions .....	43
6.2 Recommendations .....	44
<b>REFERENCES.....</b>	<b>45</b>
<b>APPENDIX A .....</b>	<b>47</b>
BACKFILL MATERIAL GRADATION .....	47
<b>APPENDIX B .....</b>	<b>48</b>
TRIAXIAL TEST RESULTS .....	48
<b>APPENDIX C .....</b>	<b>55</b>
PULLOUT TEST DATA .....	55



## **List of Tables**

Table 2.1 Summary of past laboratory pullout tests .....	15
Table 2.2 Field pullout testing (Chang et. al., 1977) .....	18
Table 3.1 Gradation requirements for select granular backfill .....	19
Table 3.2 Properties and densities of backfill materials in pullout tests.....	21
Table A. 1 Aggregate backfill gradation summary.....	47
Table C. 1 Summary of pullout test data .....	55

## List of Figures

Figure 1.1 Main components of a typical MSE wall .....	2
Figure 1.2 MSE wall applications (www.reinforcedearth.com) .....	3
Figure 1.3 Location of potential failure surface for internal stability design for inextensible reinforcements (AASHTO, 2012) .....	4
Figure 2.1 Pullout resistance mechanism on ribbed strip reinforcement (FHWA, 2001) .....	11
Figure 2.2 Default values for pullout resistance factor, $F^*$ (AASHTO, 2012).....	13
Figure 2.3 $F^*$ values for ribbed steel strip from past pullout tests ((Technical Bulletin MSE-6, 1995).....	17
Figure 3.1 Gradation curves of backfill materials .....	20
Figure 3.2 Ribbed steel strip reinforcement.....	22
Figure 3.3 RJH pullout test apparatus.....	23
Figure 3.4 Setup of displacement transducers .....	24
Figure 4.1 Compaction of the test sample .....	26
Figure 4.2 Ribbed steel strip reinforcement placed on top of the first layer .....	27
Figure 4.3 Air gauge for controlling normal stress application .....	28
Figure 4.4 Pullout load assembly.....	29
Figure 4.5 Data acquisition system.....	30
Figure 5.1 Stress-strain curves for $C_u=1.4$ .....	32
Figure 5.2 Mohr's circles for $C_u=1.4$ .....	32
Figure 5.3 Pullout force-displacement curve for aggregate with $C_u=6$ at normal stress of 69 kPa.....	34
Figure 5.4 Pullout force versus displacement curve for aggregate with $C_u=1.4$ .....	35
Figure 5.5 Pullout force versus displacement curve for aggregate with $C_u=2$ .....	35
Figure 5.6 Pullout force versus displacement curve for aggregate with $C_u=3$ .....	36
Figure 5.7 Pullout force versus displacement curve for aggregate with $C_u=4$ .....	36
Figure 5.8 Pullout force versus displacement curve for aggregate with $C_u=6$ .....	37
Figure 5.9 Pullout force versus displacement curve for aggregate with $C_u=14$ .....	37
Figure 5.10 Normal stress-pullout force curves.....	39
Figure 5.11 $F^*$ values for ribbed steel strip reinforcement in aggregate backfills .....	41

Figure 5.12 $F^*$ values versus coefficient of interface for each aggregate backfill .....	42
Figure B. 1 Stress-strain curves for $C_u=1.4$ .....	48
Figure B. 2 Mohr circles for $C_u=1.4$ .....	49
Figure B. 3 Stress-strain curves for $C_u=2$ .....	49
Figure B. 4 Mohr circles for $C_u=2$ .....	50
Figure B. 5 Stress-strain curves for $C_u=3$ .....	50
Figure B. 6 Mohr circles for $C_u=3$ .....	51
Figure B. 7 Stress-strain curves for $C_u=4$ .....	51
Figure B. 8 Mohr circles for $C_u=4$ .....	52
Figure B. 9 Stress-strain curves for $C_u=6$ .....	52
Figure B. 10 Mohr circles for $C_u=6$ .....	53
Figure B. 11 Stress-strain curves for $C_u=14$ .....	53
Figure B. 12 Mohr circles for $C_u=14$ .....	54
Figure C. 1 Pullout force-displacement curve for $C_u=1.4$ at normal stress of 25 kPa.....	56
Figure C. 2 Pullout force-displacement curve for $C_u=1.4$ at normal stress of 41 kPa .....	56
Figure C. 3 Pullout force-displacement curve for $C_u=1.4$ at normal stress of 69 kPa .....	57
Figure C. 4 Pullout force-displacement curve for $C_u=1.4$ at normal stress of 103 kPa ...	57
Figure C. 5 Pullout force-displacement curve for $C_u=1.4$ at normal stress of 138 kPa ...	58
Figure C. 6 Pullout force-displacement curve for $C_u=2$ at normal stress of 25 kPa .....	58
Figure C. 7 Pullout force-displacement curve for $C_u=2$ at normal stress of 41 kPa .....	59
Figure C. 8 Pullout force-displacement curve for $C_u=2$ at normal stress of 69 kPa .....	59
Figure C. 9 Pullout force-displacement curve for $C_u=3$ at normal stress of 25 kPa .....	60
Figure C. 10 Pullout force-displacement curve for $C_u=3$ at normal stress of 41 kPa .....	60
Figure C. 11 Pullout force-displacement curve for $C_u=3$ at normal stress of 69 kPa .....	61
Figure C. 12 Pullout force-displacement curve for $C_u=4$ at normal stress of 25 kPa .....	61
Figure C. 13 Pullout force-displacement curve for $C_u=4$ at normal stress of 41 kPa .....	62
Figure C. 14 Pullout force-displacement curve for $C_u=4$ at normal stress of 69 kPa .....	62
Figure C. 15 Pullout force-displacement curve for $C_u=6$ at normal stress of 25 kPa .....	63
Figure C. 16 Pullout force-displacement curve for $C_u=6$ at normal stress of 41 kPa .....	63
Figure C. 17 Pullout force-displacement curve for $C_u=6$ at normal stress of 69 kPa .....	64
Figure C. 18 Pullout force-displacement curve for $C_u=14$ at normal stress of 25 kPa ....	64

- Figure C. 19 Pullout force-displacement curve for  $C_u=14$  at normal stress of 41 kPa .... 65
- Figure C. 20 Pullout force-displacement curve for  $C_u=14$  at normal stress of 69 kPa .... 65
- Figure C. 21 Pullout force-displacement curve for  $C_u=14$  at normal stress of 103 kPa .. 66
- Figure C. 22 Pullout force-displacement curve for  $C_u=14$  at normal stress of 138 kPa .. 66

# **CHAPTER 1 INTRODUCTION**

This chapter provides general background of soil reinforcement and composition as well as design of mechanically stabilized earth (MSE) walls. It also covers the problem statements, objective of this research, and methodology adopted as well as the organization of this thesis.

## **1.1. Background**

FHWA (2001) provided the historical development of MSE wall system, which is summarized below. A variety of materials have been used to improve soil since the ancient time. Tree branches were used as soil reinforcement in dikes of earth in China for at least 1,000 years, and along the Mississippi River in the 1880s. Wooden pegs and bamboo or wire mesh are other materials that have been used for erosion protection and landslide mitigation in history. During medieval times, people used alternating layers of earth and logs for building fortifications. In the early 1900s, layers of metallic reinforcements were embedded in soil to reinforce the downstream slopes of earth dams. In the early 1960s, the development of the modern soil reinforcement system by Henri Vidal led to the establishment of Reinforced Earth<sup>®</sup>. This system uses steel strip reinforcement.

The primary function of reinforced soil mass is to enhance the mechanical properties (especially tensile strength) of soil by placing reinforcement layers. In other words, the reinforced soil mass behaves similar to reinforced concrete. The use of MSE wall has become widely accepted as it is a cost effective technology. The term MSE wall is generally used to describe the earth retaining systems that are constructed by adding layers of reinforcing elements into soil.

An MSE wall constructed on a foundation has four main components, namely facing unit, reinforcing elements, reinforced backfill, and retained soil. Common types of soil reinforcing elements are steel strips, welded steel grids, geogrids, and geotextile sheets. A wide range of materials used as facing units include precast concrete panels, dry cast modular blocks, welded wire mesh, wrapped-around geosynthetics, and gabions (FHWA, 2001). The select soil material placed within the reinforcement zone is referred to as reinforced backfill. In-situ soil or backfill material placed directly behind the reinforced zone is termed as a retained soil. Figure 1.1 shows the main components of a typical MSE wall system.

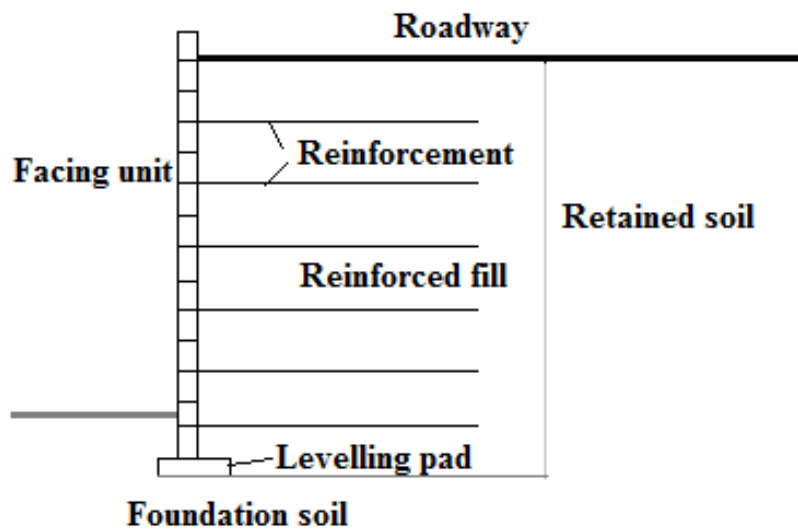


**Figure 1.1 Main components of a typical MSE wall**

MSE wall systems have been used for different applications, such as retaining walls, bridge abutments, wing walls, access ramps, and waterfront walls. The ease and speed of construction, economy, ability to tolerate differential settlement, and aesthetics are the main advantages of MSE walls, which have made them be attractive options. Figure 1.2 shows a few applications of MSE walls.



**Figure 1.2 MSE wall applications ([www.reinforcedearth.com](http://www.reinforcedearth.com))**

The design of MSE walls has been mostly based on limit equilibrium analysis where external and internal stability are required to ensure the overall stability of the MSE wall. External stability focuses on the structural integrity among main wall components, which act coherently as one unit. This analysis ensures that the MSE wall has sufficient factors of safety against potential failure modes, such as sliding, overturning, bearing, and global failure. In addition to the external stability, internal stability analysis is needed to ensure the MSE wall has sufficient factors of safety against rupture and pullout of reinforcement and connection failure between reinforcement and wall facing.

For internal stability analysis against pullout failure, the reinforced fill is divided into active and resisting zones as shown in Figure 1.3. Pullout failure is the outward sliding of the reinforcement from the resisting zone. Therefore, the portion of the reinforcement embedded in the resisting zone,  $L_e$ , is used for pullout resistance determination. Pullout tests have been commonly used to evaluate reinforcement pullout resistance.

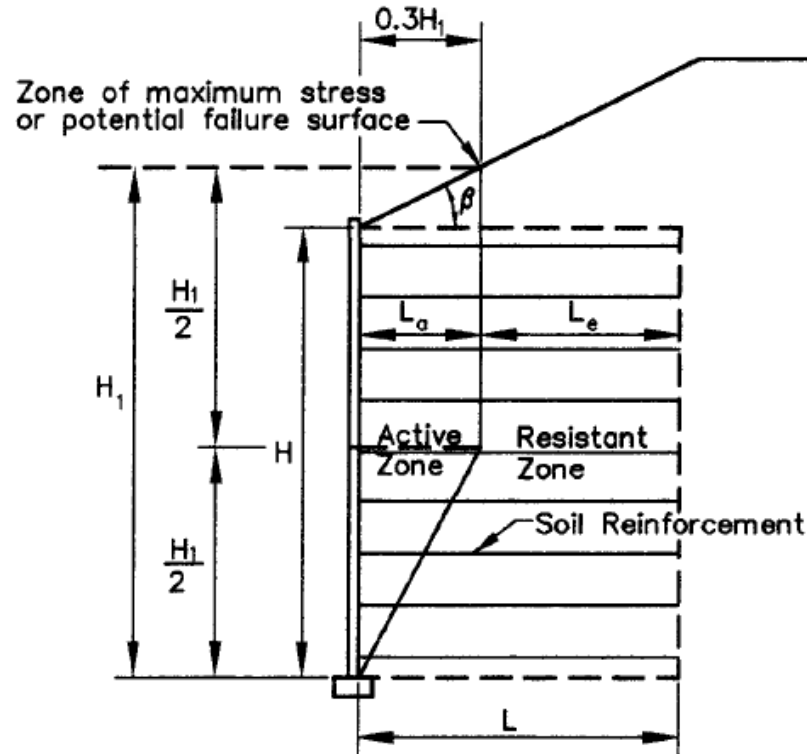


**Figure 1.3 Location of potential failure surface for internal stability design for inextensible reinforcements (AASHTO, 2012)**

## 1.2. Research Problem Statement

MSE walls have been commonly used in Kansas to support bridge abutments, sound barrier walls, and other structures. Within MSE walls steel strips are often used as reinforcement to stabilize aggregate backfill through anchorage. The anchorage capacity of strip reinforcement depends on its tensile strength and pullout resistance in aggregate. The pullout resistance of strip reinforcement is dependent on the pullout resistance factor between strip reinforcement and aggregate. AASHTO design guidelines (AASHTO, 2012) provide a formula to estimate the pullout resistance factor for strip reinforcement in aggregate with a uniformity coefficient  $C_u \geq 4$  where the uniformity coefficient is defined as the ratio of the particle size at 60% finer to that at 10% finer. AASHTO design



guidelines (AASHTO, 2012) require pullout tests to determine the pullout resistance factor of strip reinforcement in aggregate with a uniformity coefficient of  $C_u < 4$ .

This requirement has resulted in disqualification of a large amount of aggregate produced by the quarries in Kansas for MSE wall construction. If the aggregate is re-processed to meet the uniformity requirement, the cost of aggregate will be increased. Alternatively, pullout tests of strip reinforcement can be performed to determine the pullout resistance factor. Unfortunately, no commercial laboratory is readily available in Kansas to provide such pullout testing service. Strip reinforcement and aggregate have to be sent to a couple of specialty laboratories in the nation, which will increase the cost and potentially delay construction. Therefore, there is a great need to verify the existing AASHTO pullout resistance formula (AASHTO, 2012) for Kansas aggregates with coefficient of uniformity less than 4 or develop a new formula that is applicable to these aggregates.

### **1.3. Research Objective**

The objective of this research was to evaluate the pullout resistance of steel strip reinforcement embedded in aggregate with a uniformity coefficient  $C_u < 4$  and verify the existing AASHTO pullout resistance formula (AASHTO, 2012) for Kansas aggregates or develop a new formula that is applicable to these aggregates. Therefore, a series of pullout tests were conducted with Kansas aggregates of different uniformity coefficients in the Geotechnical Engineering Laboratory at the University of Kansas.

## **1.4. Research Approach**

This research first identified potentially usable aggregates and steel strip reinforcement in Kansas. Six types of aggregates with different uniformity coefficients from the quarries in Kansas and one type of ribbed steel strip reinforcement from the manufacturer, Reinforced Earth Company®, were collected. To determine the gradations of the aggregates, sieve analyses were conducted using a large sieve machine, and the uniformity coefficients were calculated for all types of aggregates. Additionally, the angle of friction for each type of aggregate was determined using large triaxial shear tests in the Geotechnical Engineering Laboratory at the University of Kansas. Standard density tests were conducted to obtain the minimum and maximum dry densities of all aggregates. After the physical characteristics of the aggregates were identified and confirmed, pullout tests were performed on strip reinforcement embedded in these aggregates at three different normal stresses. Finally, pullout test data were analyzed to estimate the pullout resistance factors of the steel strip reinforcement embedded in six different aggregate backfills under different normal stresses.

## **1.5. Thesis Organization**

This thesis includes six chapters. Chapter 1 presents the brief introduction to this study, which comprises background, problem statement, research objective, research methodology, and thesis organization. Chapter 2 provides the literature review on past research work related to this study, which includes stress transfer mechanisms in MSE walls, guidelines for pullout resistance determination, and both laboratory and field pullout testing performed by others. Chapter 3 discusses the test materials and apparatus. Chapter

4 describes the test procedure and data acquisition system used in this study. The test results and data analyses are discussed in Chapter 5 of this thesis. Chapter 6 presents the conclusions and recommendations based on the test results and analyses.

## **CHAPTER 2 LITERATURE REVIEW**

As explained in Chapter 1 of this thesis, people have long realized that adding appropriate reinforcing elements into soil can increase soil resistance. The modern soil reinforcement technology was developed as Reinforced Earth five decades ago. Mechanically stabilized earth (MSE) wall was part of this development. The use of MSE walls has become widely accepted as a cost effective technology to support bridge abutments, sound barrier walls, and other structures. A variety of MSE reinforcements have been used since the introduction of the modern soil reinforcement system. MSE walls with steel strips are often used as reinforcement to stabilize aggregate backfill. Granular soils are considered to be ideally suitable backfill for MSE structures.

With increasing demand of MSE wall applications, a number of researchers have conducted studies to evaluate the backfill-reinforcement interaction. Some of these investigations have been performed on steel strip reinforcement. Pullout tests have been commonly adopted to investigate the factors that govern pullout resistance of reinforcement in soil.

This chapter presents a literature review on related research work done by others in the past, including the mechanisms that govern the interaction between soil and reinforcement, the standard guidelines for estimating pullout resistance in the absence of pullout test results, and past laboratory and field pullout tests relevant to this study.

### **2.1 Stress Transfer Mechanism**

The French architect and engineer, Henri Vidal, was credited for the development of the modern soil reinforcement technology in 1960s (FHWA, 2001). Vidal (1969) recognized

that the capability of an earth mass to withstand tensile stresses can be enhanced by embedding strip reinforcements. He realized that the bond developed within the reinforced earth arises from the friction between the reinforcing element and particles. Hence, he recommended that proper bonding is required at the soil-reinforcement interface so that slippage will be avoided.

Several investigations have been carried out on alternative soil reinforcement materials other than the steel strip reinforcement. As a result, the welded wire soil reinforcement was introduced and later gained widespread applications. Chang, Hannon, and Forsyth (1977) performed experimental tests to evaluate the pullout resistance of strip and welded wire mesh-type reinforcements. This study reported that plain bar-mesh reinforcement resulted in pullout resistance approximately six times that of strip-type reinforcement with the same reinforcement surface area in gravely sand soil. Peterson (1980) performed a comprehensive study on the mechanisms that govern the pullout resistance of welded wire mesh. He found two separate mechanisms contributing to the pullout resistance in welded wire mesh, which are *friction* between longitudinal wires and soil particles and *anchorage* of transverse wires embedded in the soil. As shown in Equations 2.1 and 2.2, Peterson (1980) suggested formulas for estimating the frictional resistance,  $F_t$ , along single longitudinal wire of length  $l$ , and bearing (anchorage) resistance,  $P_b$ , for a single traverse wire in cohesionless backfills, respectively.

$$F_t = \sigma_v(\pi dl)\tan\delta \quad \text{Equation 2.1}$$

$$P_b = \sigma_v d N_q \quad \text{Equation 2.2}$$

where  $\sigma_v$  = normal stress,  $\delta$  = backfill-reinforcement friction angle,  $d$  = diameter of reinforcement wire,  $N_q$  = bearing factor which depends on internal friction angle,  $\phi$ , and given as follows:

$$\text{For general shear failure,} \quad N_q = e^{\pi \tan \phi} \tan^2 \left( 45 + \frac{\phi}{2} \right) \quad \text{Equation 2.3}$$

$$\text{For punching shear failure,} \quad N_q = e^{(\frac{\pi}{2} + \phi) \tan \phi} \tan \left( 45 + \frac{\phi}{2} \right) \quad \text{Equation 2.4}$$

The FHWA manual (FHWA, 2001) stated that the stress transfer mechanism between soil and reinforcement is governed by friction and/or passive resistance, depending on reinforcement geometry. Friction develops at the locations where relative shear displacement occurs between the reinforcement surface and backfill soil. Steel strips, longitudinal bars of welded steel grids, geotextiles and geogrids have reinforcing elements that generate pullout resistance through friction. Passive resistance occurs through the development of bearing-type stresses on reinforcing elements oriented normal to the direction of movement. Passive resistance is generally considered to be the primary resistance for rigid geogrids and wire mesh reinforcements. The transverse ridges on ribbed strip reinforcement also provide some passive resistance. Figure 2.1 illustrates the frictional and passive resistance mechanisms of the ribbed steel strip reinforcement under pullout force.

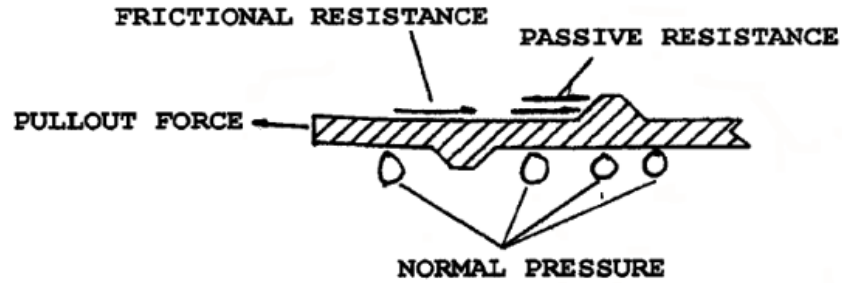


**Figure 2.1 Pullout resistance mechanism on ribbed strip reinforcement (FHWA, 2001)**

Moreover, the reinforcement characteristics that affect the contribution of each transfer mechanism include surface roughness, normal effective stress, grid aperture, thickness of transverse members, and elongation characteristics of the reinforcement. Equally important for interaction development are the soil characteristics, which include grain size, grain size distribution, particle shape, density, water content, cohesion, and stiffness (FHWA, 2001).

## **2.2 Guidelines for Pullout Resistance Determination**

The ultimate tensile load required to generate the outward movement of the reinforcement through the reinforced soil mass is defined as the pullout resistance of reinforcement. Several approaches and design equations have been established and are currently used to estimate the pullout resistance by considering frictional, and/or passive resistance. FHWA (2001) introduced a definition of pullout resistance based on a pullout resistance factor,  $F^*$ . This single parameter  $F^*$  combines the contribution of the two separate stress transfer mechanisms to pullout resistance. According to the AASHTO LRFD Bridge Design Specifications (AASHTO, 2012) or the FHWA manual (2001), the pullout resistance,  $P_r$ ,

of the reinforcement per unit width of reinforcement is calculated using the following generalized Equation 2.5:

$$P_r = F^* \alpha \sigma_v C L_e \quad \text{Equation 2.5}$$

where  $L_e$  = length of reinforcement in the resisting zone,  $F^*$  = pullout friction factor,  $\alpha$  = scale effect correction factor (for steel reinforcement,  $\alpha = 1$ ),  $\sigma_v$  = vertical overburden stress at the reinforcement level,  $C$  = overall reinforcement surface area geometry factor based on the gross perimeter of the reinforcement (equal to 2 for strip, grid, and sheet-type reinforcements).

Generally, it is more reliable to evaluate the pullout resistance of reinforcement in backfill material used in a specific project by conducting pullout tests. However, it may practically not be possible to perform pullout tests as the specific backfill source may not be known at the time of wall design. Thus, in common design practice, the pullout resistance of reinforcement is estimated using the pullout resistance factor,  $F^*$ . The AASHTO LRFD Bridge Design Specifications (AASHTO, 2012) provides default values of pullout resistance factor  $F^*$  for standard backfill materials with a uniformity coefficient  $C_u \geq 4$ . In the absence of site specific pullout test data, the semi-empirical relationships in Figure 2.2 may be used to estimate the pullout resistance factor,  $F^*$ , which can be used to calculate pullout resistance of reinforcement for internal stability analysis of walls.



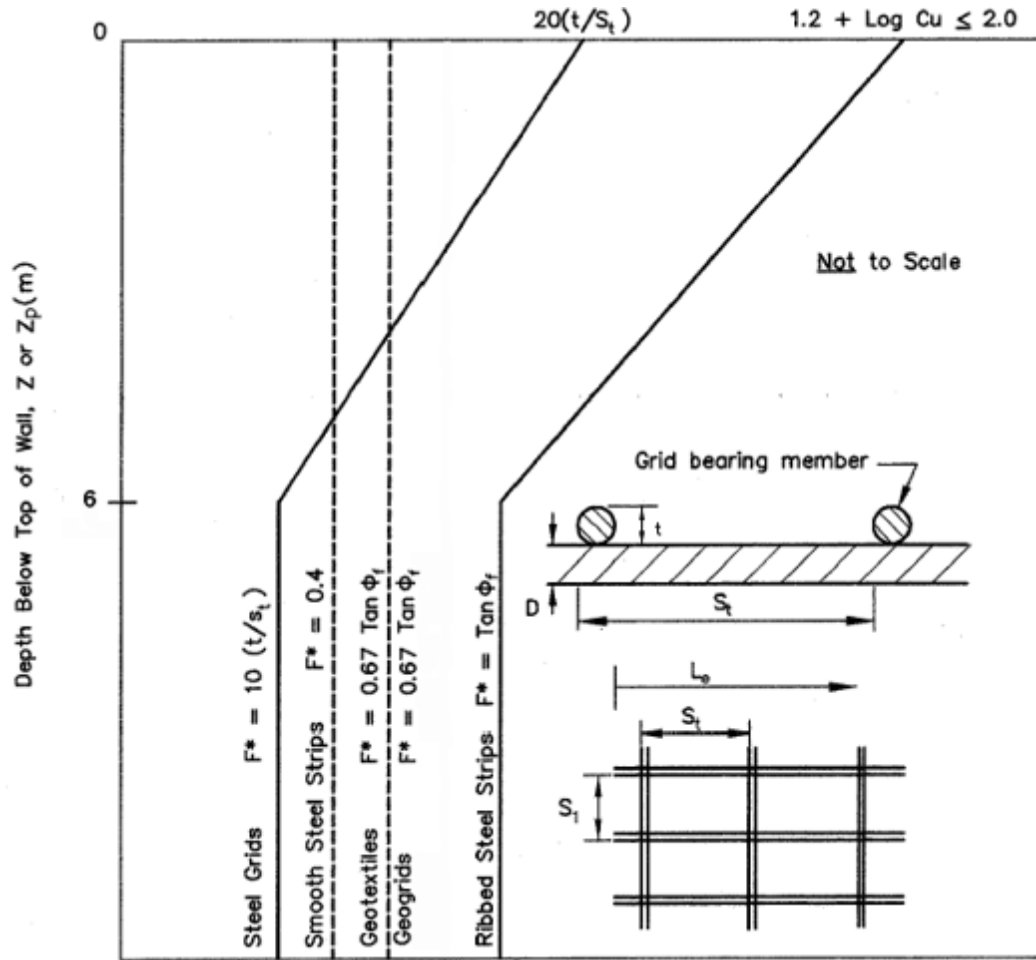


**Figure 2.2 Default values for pullout resistance factor,  $F^*$  (AASHTO, 2012)**

The pullout resistance factor,  $F^*$ , for steel ribbed reinforcement, can be estimated as follows:

$$F^* = \tan \rho = 1.2 + \log C_u \leq 2 \text{ at the top of the wall} \quad \text{Equation 2.6}$$

$$F^* = \tan \phi \text{ at a depth of 6m and below} \quad \text{Equation 2.7}$$

where  $C_u$  is the uniformity coefficient of the backfill and  $\phi$  is the angle of internal friction of the backfill. If the specific  $C_u$  for the backfill is unknown at the time of MSE wall design, a  $C_u$  of 4 should be assumed (i.e.,  $F^* = 1.8$  at the top of the wall), for backfill meeting the AASHTO (2010) requirements.

## **2.3 Past Pullout Tests**

The following sections summarize the laboratory and field pullout tests performed by others in the past.

### **2.3.1 Laboratory Pullout Tests**

A number of laboratory tests have been performed to evaluate the pullout resistance of inextensible metallic (steel) and extensible (geosynthetic) reinforcements from soil. Lawson, Jayawickrama, Wood, and Surles (2013a) provided a summary of literature review on 22 laboratory pullout tests performed on inextensible metallic reinforcements prior to TxDOT project 0-6493. According to this literature summary, the backfill materials used in the pullout tests ranged from silt and weathered clay with low plasticity to granular soil or crushed stone. However, most of the laboratory tests used granular soils as backfill.

The test data for ribbed steel reinforcement from past laboratory pullout tests are limited. Table 2.1 presents the summary of the laboratory pullout tests conducted on steel strip reinforcements embedded in granular backfill. Table 2.1 was modified from that in Lawson et al. (2013a). Although some of the pullout tests investigated different types of reinforcements at the same time, information related to strip reinforcement is included in Table 2.1.

**Table 2.1 Summary of past laboratory pullout tests**

<b>Reference</b>	<b>Backfill</b>	<b>Reinforcement</b>	<b>Pullout box</b>	<b>Normal Stress (kPa )</b>	<b>Pullout Load Application</b>
Chang et al. (1977)	Poorly-graded gravelly sand	Steel strip: 60 mm wide, 3 mm thick, and 1370 mm long	91.4 mm wide, 1372 mm long, and 457 mm high	69 (by hydraulic jack)	By a hydraulic jack at a strain rate of 0.05 mm/min
Lee and Bobet (2005)	Clean sand, and silty sand	Steel strip: 50 mm wide, 3 mm thick, and 750 mm effective length	Two chambers: (a) soil chamber of 400 mm wide, 1000 mm long, 500 mm high; and (b) water chamber*	30, 100, and 200 (by air bag)	By an electric hydraulic ram at a strain rate of 1mm/min for drained and 10 mm/min for undrained tests
Rathje et al. (2006)	Crushed concrete and recycled asphalt pavement aggregate	Ribbed steel strip: 50 mm wide, 450 mm long, about 4 mm thick, and 3 mm high ribs	500 mm wide, 500 mm long, and 337.5 mm high	10 to 130 (by air bag)	By a pneumatic piston with a strain rate of 1 mm/min
Lawson et al. (2013a)	**Type A and Type B	Ribbed steel strip: 50 mm wide, 1.2 m, 1.8 m, 2.4 m, and 3.6 m long, and 4 mm thick.	3.7 m wide, 3.7 m long, and 1.22 m high	26 to 270 (by hydraulic jack)	By a hollow core hydraulic jack at a strain rate ranging 1.25 to 6 mm/min

\*Water chamber is a box used for water supply to saturate the soil and maintain constant water pressure in the soil chamber during pullout testing.

\*\*Type A: gravelly backfill with uniformity coefficient of 12-180, which is classified as GW/GP/GP-GM.

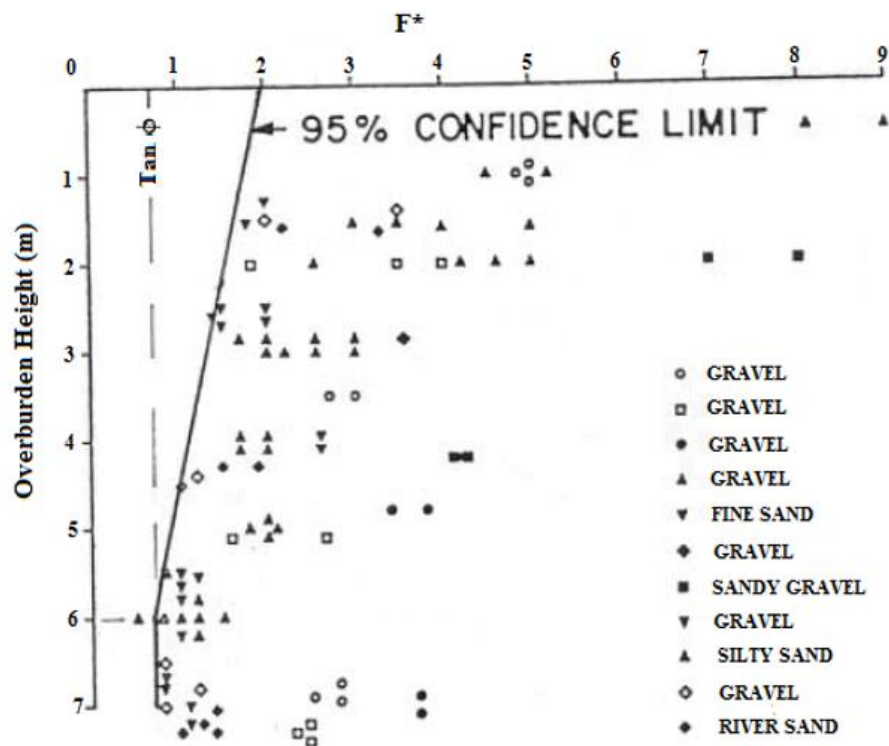
Type B: sandy backfill with uniformity coefficient of 4.4-7.0, which is classified as SP-SM (Lawson et al., 2013a and 2013b).

Table 2.1 shows that all the pullout tests were carried out on strip reinforcements embedded in granular soils except the test conducted by Rathje et al. (2006), in which crushed concrete and recycled asphalt pavement aggregate were used as backfill. According to Lawson et al. (2013a), in most of the tests, no adequate information was given whether these backfill materials satisfied the gradation requirements set by the AASHTO LRFD Bridge Construction Specifications (AASHTO, 2010). The backfill materials used by Lawson et al. (2013a) marginally satisfied the requirements for MSE wall select backfill as specified in the AASHTO specifications (AASHTO, 2010). Also, in their study, the uniformity coefficients were provided for each backfill material. The test performed by Rathje et al. (2006) primarily aimed at investigating the suitability and sustainability of crushed concrete and recycled asphalt pavement aggregate to be used as MSE wall backfills; not the internal stability of the backfill-reinforcement mass. Although Lawson et al. (2013a) performed the pullout tests on two types of backfill materials (Types A and B), the main objective of their study was to determine pullout resistance factors applicable to specific backfill-reinforcement combinations used by TxDOT. Therefore, none of the above tests focused on investigating the effect of backfill material gradation on the pullout resistance of the reinforced mass. Furthermore, most of the past research works were performed either on backfill materials with a uniformity coefficient  $>4$  or backfill without sufficient gradation information.

Different sizes of test boxes were used in the above pullout tests. The smallest test box was the one used by Rathje et al. (2006) with dimensions of 500 mm wide x 500 mm long x 337.5 mm high; whereas the largest test box used by Lawson et al. (2013a and 2013b) had dimensions of 3.7 m wide x 3.7 m long x 1.22 m high. Inflated air bag and

hydraulic jack against a reaction frame are two common ways used to simulate the overburden stresses. In the above tests, except the tests by Rathje et al. (2006), hydraulic jack was used to apply the pullout load.

As shown in Figure 2.3, the Reinforced Earth Company (Technical Bulletin MSE-6, 1995) presented a summary of the relationship of the pullout resistance factors,  $F^*$ , versus the depth of fill based on the data obtained from past laboratory pullout tests on strip reinforcement embedded in granular soils. Even though most of the data points lied to the right side of the 95 % confidence limit (equivalent to the AASHTO limit line), a few of them were plotted to the left or on the confidence limit. Once again, it should be noted that there was no sufficient information about the gradation of the backfill materials.



**Figure 2.3  $F^*$  values for ribbed steel strip from past pullout tests ((Technical Bulletin MSE-6, 1995)**

Laboratory pullout tests performed by Lawson et al. (2013a) showed that the pullout resistance factors,  $F^*$ , for ribbed strip reinforcements embedded in granular backfill are considerably higher than the default  $F^*$  values provided by the AASHTO. Moreover, the pullout resistance factors,  $F^*$ , for ribbed strip reinforcements embedded in the gravelly backfill (Type A) were found to be significantly higher than those embedded in the sandy backfill (Type B).

### 2.3.2 Field Pullout Tests

Limited field pullout tests have been conducted to determine steel strip pullout resistance. Chang et al. (1977) carried out field tests on pullout resistance of strip reinforcement embedded in decomposed granite in a reinforced earth wall constructed on Cal-39 in the San Gabriel Mountains. The summary of this field study is presented in Table 2.2.

**Table 2.2 Field pullout testing (Chang et. al., 1977)**

Backfill	Reinforcement	Depth of fill	Pullout load
Decomposed granite	Galvanized steel strips of 60 mm wide, 1.5, 3, 4.5, 6.9, and 13.8 m long, and 3 mm thick; additional dummy steel strips used	1.5, 3, and 4.5 m long strips embedded at depths of 2.25, 3.72, and 5.46 ft, respectively; three 6.9 and 13.8 m long strips at depths of 5.4, and 11.4 m, respectively	No details provided

In this study, smooth steel strips were used instead of ribbed strips. According to Lawson et al. (2013a), most of the pullout resistance factors,  $F^*$ , estimated based on the field test data were higher than the default values provided by the AASHTO (2012). However, some of the field measured  $F^*$  lied to the left of the reference line for smooth steel strips recommended by the AASHTO (2012).

## CHAPTER 3 TEST MATERIALS AND APPARATUS

This chapter describes the test materials and the test apparatus used in this study, including the characteristics and specifications of the backfill materials, the type of steel reinforcement, and the details of the newly developed pullout test apparatus.

### 3.1 Backfill Material

The pullout resistance of reinforcement is influenced by engineering properties of a backfill material. Granular soils are considered to be suitable backfill for MSE structures because of their high strength, stiffness, and permeability. The AASHTO LRFD Bridge Construction Specifications (AASHTO, 2010) and the FHWA manual (FHWA, 2001) specify that all backfill material used in MSE walls shall be free from organic or other deleterious materials and conform the gradation requirements as provided in Table 3.1. In addition, an angle of internal friction of at least 34 degrees is recommended for select backfill material.

**Table 3.1 Gradation requirements for select granular backfill**

<b>U.S. Sieve Size</b>	<b>Percent Passing: FHWA-NHI-00-043</b>
102 mm	100
0.425mm (No. 40)	0-60
0.075mm (No. 200)	0-15

As mentioned in Chapter 1, the objective of this study was to evaluate the effect of aggregate uniformity coefficient on the pullout resistance of ribbed strip reinforcement embedded in aggregates. Six types of aggregates with gradation curves as shown in Figure

3.1 were used for pullout tests, which had uniformity of coefficients of 1.4, 2, 3, 4, 6, and 14, respectively. These aggregates were obtained from the Bonner Spring Quarry, APAC-Kansas, Inc. Particle size distribution tests (ASTM Standard D422, 2007) were conducted to verify their compliance with the recommended gradation requirements. All these aggregates satisfy the AASHTO MSE wall select granular fill gradation requirements (AASHTO, 2010) and the KDOT specification (KDOT, 2007).

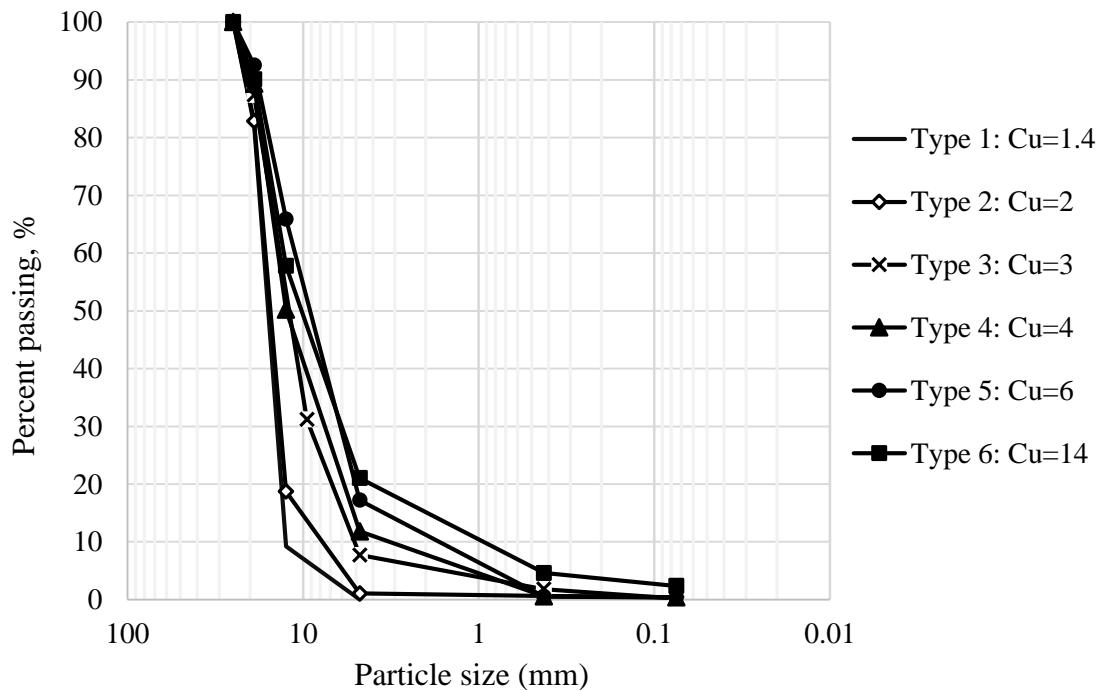


### Figure 3.1 Gradation curves of backfill materials

The friction angle of each aggregate backfill was determined using standard triaxial compression tests (ASTM D7181, 2011). All the backfill materials used in this study were gravelly type. The maximum index density method (ASTM D4253, 2000a) was initially used to determine the maximum dry densities of the aggregates. However, this method resulted in lower dry densities as compared with those determined by the standard Proctor compaction tests (ASTM D698-12e1, 2012). Considering the fact that aggregates are



mostly compacted under a dry condition by vibratory rollers in field, dry compaction densities are more representative to field conditions. Therefore, the maximum dry density of the aggregate determined by the standard Proctor compaction was used to prepare the pullout test samples. However, the minimum dry densities were determined using the minimum index density method (ASTM Standard D4254, 2000b). Table 3.2 summarizes the physical properties, the USCS classification, the angle of friction, and the degree of compaction of the aggregates used in the pullout tests.

**Table 3.2 Properties and densities of backfill materials in pullout tests**

<b>Property</b>	<b>Type 1</b>	<b>Type 2</b>	<b>Type 3</b>	<b>Type 4</b>	<b>Type 5</b>	<b>Type 6</b>
Coefficient of uniformity, $C_u$	1.4	2	3	4	6	14
Coefficient of curvature, $C_c$	1.0	1.44	1.12	1.04	1.82	2.57
USCS classification	GP	GP	GP	GW	GW	GW
Maximum dry unit weight ( $\text{kN/m}^3$ )	15.8	16	17.1	17.4	17.6	18.6
Minimum dry unit weight ( $\text{kN/m}^3$ )	12.7	12.6	13.4	14.5	13.6	14.9
Angle of friction (deg)	46	49	47	47	49	46
Relative compaction (%)	94	94	93	94	93	93
Relative density (%)	75	75	75	75	75	70

### **3.2 Reinforcement**

This experimental study evaluated the pullout resistance of galvanized ribbed steel strip reinforcements of 1500 mm long, 50 mm wide and 4 mm thick, which were provided by the Reinforced Earth Company. The strip reinforcement has ribs of 3 mm in height on both the top and bottom of the strip with a spacing as shown in Figure 3.2. The effective embedded length,  $L_e$ , for all pullout tests was 1.2 m.

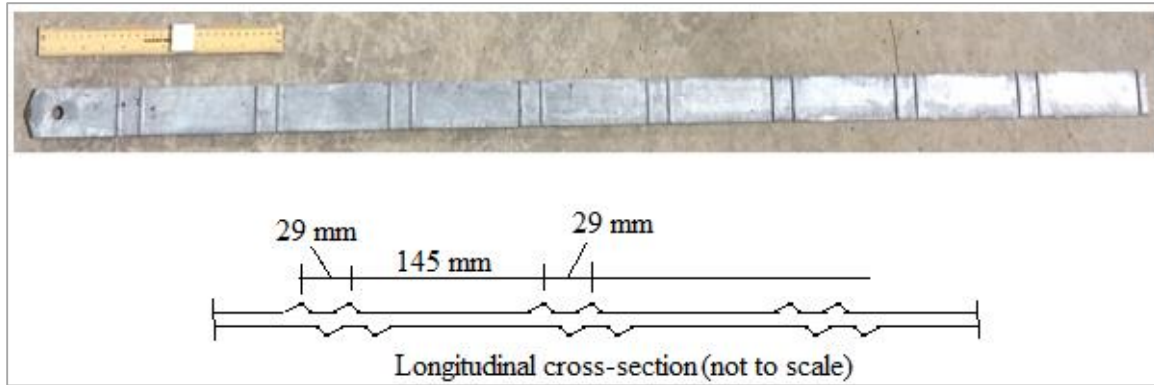


**Figure 3.2 Ribbed steel strip reinforcement**

### **3.3 Pullout Test Apparatus**

The common approach to evaluate the pullout resistance of soil reinforcements is to use a pullout box. ASTM D6706 (2001) recommends that the minimum dimensions of a large-scale pullout test box should be 610 mm long x 460 mm wide x 305 mm deep. If required, the dimensions of the box should be increased in such a way that the minimum width of the box is greater of 20 times the D<sub>85</sub> of the soil or 6 times the maximum soil particle size; and the box length should exceed 5 times the maximum size of the geogrid aperture size. In this experimental study, a newly developed pullout box was used. This box was designed and fabricated in the Geotechnical Engineering Laboratory at the University of Kansas, and was designated as the “RJH” pullout box according to the initials of last names of the developers (S.M. Rahmaninezhad, Y. Jiang, and J. Han). The box is made of steel and has inner dimensions of 1500 mm long x 600 mm wide x 600 mm high, which exceed those recommended by the ASTM. The pullout box has a 45 mm high slot on the front wall. In order to minimize the arching effect during a pullout test, 150 mm long sleeve was fixed on the inner side of the front wall and right above the slot. Figure 3.3 shows the new RJH pullout box.



**Figure 3.3 RJH pullout test apparatus**

In this pullout box apparatus, a uniform normal stress is applied to the embedded earth reinforcement using an air bag. The normal stress simulates the field overburden stress. The pullout load is applied using a double acting hydraulic jack (Model HD-3008) with a maximum capacity of 300 kN, which was manufactured by the BVA Hydraulics. This jack is mounted on a steel frame and connected to a main hydraulic pump. The pull force is transmitted to the strip reinforcement through a high tensile strength metal extension rod. The strip reinforcement is connected to the extension rod using a pin mechanism. An S-shape load cell with a maximum capacity of 50 kN is placed next to the hydraulic jack to measure the pullout force.

In this research project, two displacement transducers were used to measure the displacements of the ribbed strip reinforcement. One displacement transducer was fixed at the back end of the strip reinforcement by extending a metal string using a pin

connection. The second displacement transducer was mounted on the metal frame that supported the pullout load assembly. The displacement transducers used in this research had two displacement ranges: 0 to 100 mm and 0 to 50 mm. Figure 3.4 shows the setup of the displacement transducers.



**Figure 3.4 Setup of displacement transducers**

## **CHAPTER 4 TEST PROCEDURE AND DATA ACQUISITION**

This chapter describes the test procedure and data acquisition system adopted in this study.

### **4.1 Pullout Test Procedure**

The test procedure adopted for the pullout tests on ribbed steel strip reinforcement had four steps: (1) test sample preparation, (2) application of normal stress, (3) application of pullout load, and (4) the backfill and the reinforcement were removed from the test box and cleaned up for the next test. This procedure was repeated for each backfill material under one normal stress. A total of 22 pullout tests were conducted, which included six backfill materials under different normal stresses.

#### **4.1.1 Test Sample Preparation**

The first step in each pullout test was to prepare a test sample. Preparation of the test sample comprised filling of the test box with the backfill material, placement of a steel strip, compaction of the reinforced backfill, and instrumentation. Proper handling of each procedure of the test sample preparation would significantly affect test results. Thus, great care was given for this step.

The weight of aggregate required to achieve the target density was initially prepared. After that, the backfill material was placed in the box in two lifts. Each lift was compacted using an air backfill tamper with a circular base diameter of 125 mm until the compacted lift thickness of at least 150 mm was attained. Since all the backfill materials used in this study were coarse aggregates (gravel), the sample was compacted until the

required degree of compaction was achieved. The appropriate number of passes needed to achieve the required relative density was determined by observation in early stages of the tests. Figure 4.1 shows compaction of the test sample.



**Figure 4.1 Compaction of the test sample**

As shown in Figure 4.2, the strip reinforcement was embedded in the middle of backfill and attached to the pullout load assembly. The effective embedment length of the reinforcement was measured from the inner edge of the sleeve to the rear end of the reinforcement. The depth of the backfill above and below the reinforcement was maintained to be at least 150 mm, which met the ASTM recommendation (ASTM D6706, 2001).



**Figure 4.2 Ribbed steel strip reinforcement placed on top of the first layer**

As part of the test preparation, all the instruments, including the displacement transducers, the load cell, and the pressure gauge were fixed at their right locations. These instruments, except the pressure gauge, were connected to the data recorders and the computer. Every instrument was inspected to ensure that proper installation was achieved before proceeding to the next steps of the test procedure.

#### **4.1.2 Application of Normal Stress**

The normal stress was applied with a pressurized air bag placed on the top of compacted backfill. Air pressure was supplied by the laboratory compressed air system and controlled by the air pressure gauge as shown in Figure 4.3. To create a uniform distribution of normal stress over the backfill as well as to protect the air bag from damage, a 3 mm thick geomembrane sheet was placed directly below the air bag. In this study, each type of aggregate was tested under normal stresses of 25, 41 and 69 kPa to simulate reinforcements



placed at different depths of fill. Additionally, aggregate backfills with  $C_u=1.4$  and 14 were tested under normal stresses of 103 and 138 kPa to further evaluate the pullout resistance at higher depths.

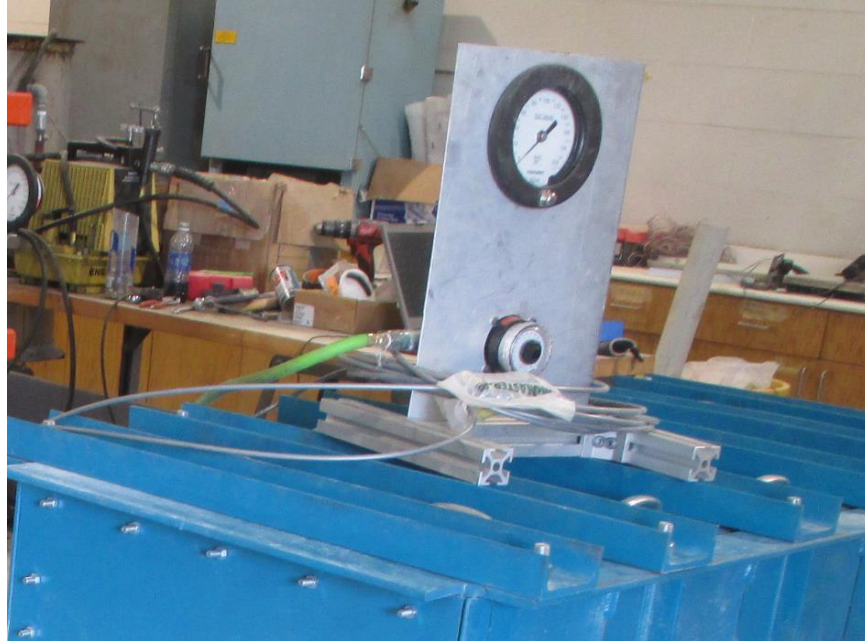


**Figure 4.3 Air gauge for controlling normal stress application**

#### **4.1.3 Application of Pullout Load**

Once the normal stress distribution throughout the entire soil mass became stable, and the load assembly was set up, the pullout load was applied using a double acting hydraulic jack at a strain rate ranging 10 to 15 mm/min. The hydraulic jack was connected to a hydraulic pump using two hoses. A check valve was installed to one of the hoses to regulate the pressure applied to the hydraulic jack.

The applied pullout load and displacements in the two displacement transducers were monitored until ultimate pullout resistance was reached, i.e., the load reading started to



decrease considerably. Figure 4.4 shows the pullout load assembly, which consists of the hydraulic jack, the load cell, and the metal pulling rod mounted on the steel frame.

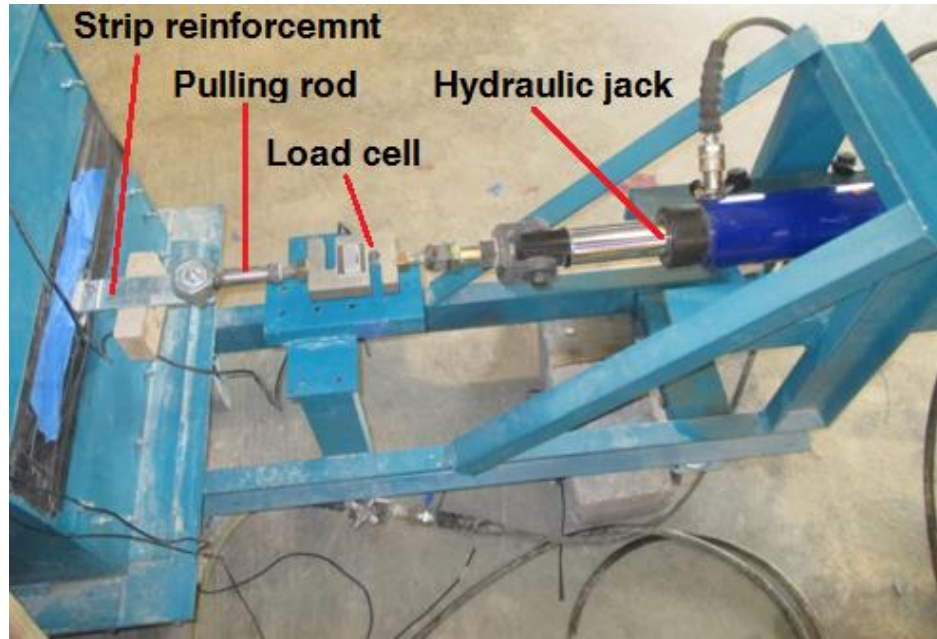


**Figure 4.4 Pullout load assembly**

## **4.2 Data Acquisition**

Once the whole pullout test was set up, all sensors were activated to allow the data acquisition system to start recording data. Data collected during the pullout test included: (1) pullout force, measured with the load cell (2) normal stress applied to the soil mass, and (3) longitudinal displacements, measured using two displacement transducers.

A Smart Dynamic Strain Recorder was used to record the data from displacement transducers and load cell. The normal stress applied to the soil mass through the air bag was monitored by the pressure gauge. Figure 4.5 shows the data acquisition system used in this study.



**Figure 4.5 Data acquisition system**

## **CHAPTER 5 TEST RESULTS AND DATA ANALYSIS**

This chapter presents the laboratory triaxial and pullout test results. Triaxial tests were carried out to determine the internal friction angle of the each backfill material. Laboratory pullout tests were conducted on ribbed steel strip reinforcements embedded in six different aggregates. Each test resulted in a calculated pullout resistance factor,  $F^*$ , for the particular reinforcement-backfill combination under a specific normal stress. This chapter also includes the comparisons of the calculated  $F^*$  values from this study with those in the AASHTO specifications (AASHTO, 2012).

### **5.1 Triaxial Test Results**

Consolidated drained triaxial compression tests (ASTM D7181, 2011) were performed to determine the strength parameters of the aggregate backfills. Each backfill material was tested under three confining stresses (69, 103, and 138 kPa). As presented in Table 3.2 of chapter 3, the internal friction angles of the six aggregate backfills were found to be within a range of 46-49°. These friction angles correspond to the normal stresses at 5 % strain. Figures 5.1 and 5.2 show stress-strain curves and Mohr's circles, respectively, for one backfill aggregate. All triaxial test results are provided in the APPENDIX B of this thesis.

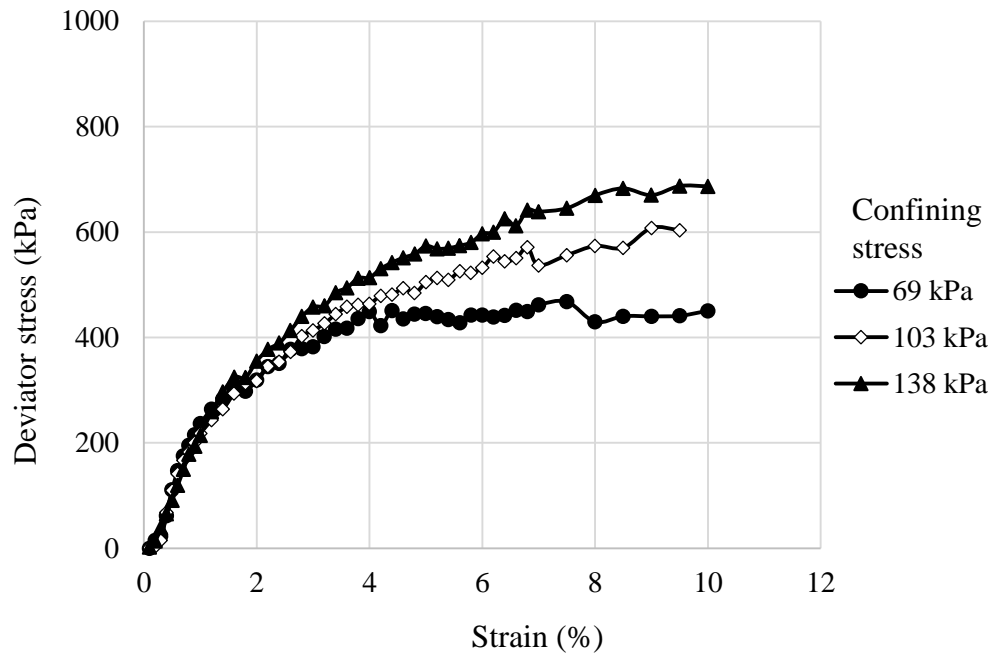


**Figure 5.1 Stress-strain curves for Cu=1.4**

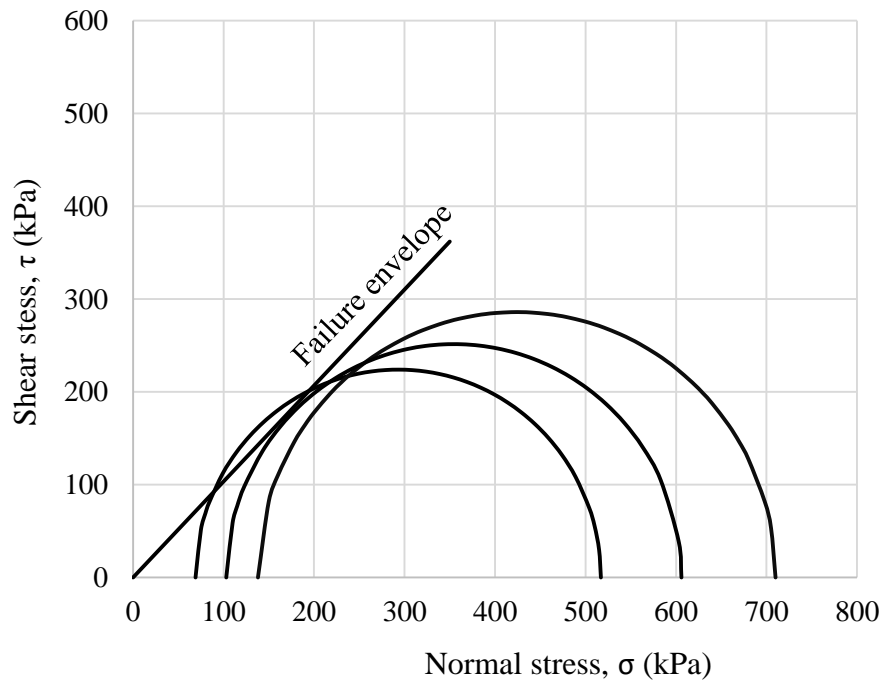


**Figure 5.2 Mohr's circles for Cu=1.4**

## **5.2 Pullout Test Results**

The test data obtained from the pullout tests included normal stress, pullout force, and displacement at the back and front ends of the strip reinforcement. Test results were plotted and analysed in the following sections of this chapter.

## **5.3 Pullout Force and Displacement**

Application of a pullout load generates an outward displacement of a particular reinforcement from soil mass in a pullout test. The ultimate pullout load is often defined as pullout resistance. The displacements of the strip reinforcement were measured at the back and front ends, which were almost identical for most of the tests, because of the use of inextensible metallic reinforcement. Figure 5.3 shows the pullout force-displacement curves corresponding to back and front displacements for the aggregate with  $C_u=6$  under the normal stress of 69 kPa. All curves are included in APPENDIX C of this thesis.

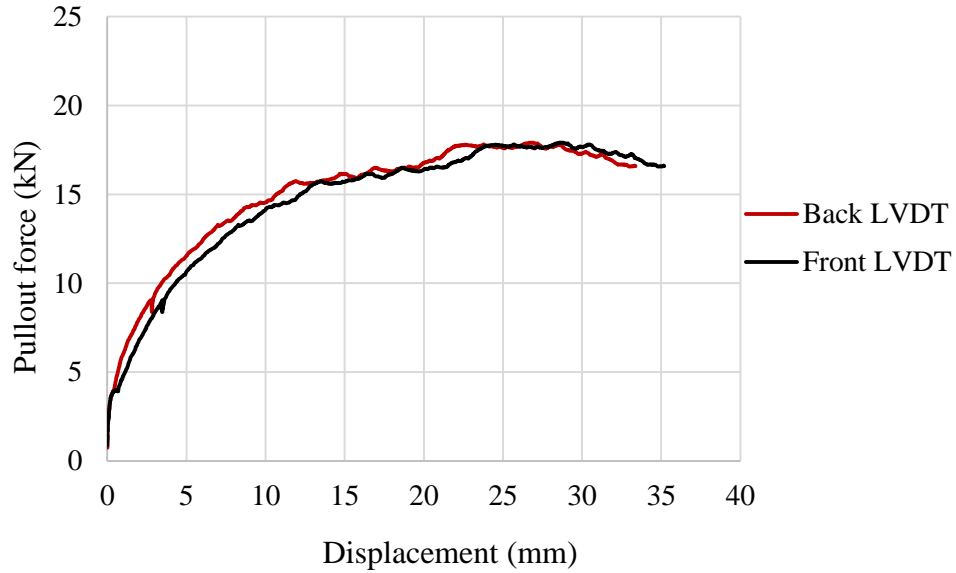


**Figure 5.3 Pullout force-displacement curve for aggregate with  $C_u=6$  at normal stress of 69 kPa**

After the pullout forces and their corresponding displacements were obtained, they were presented graphically to evaluate the ultimate pullout force. The front displacement was used for data analysis. Figures 5.4 to 5.9 show the pullout test results for six reinforcement-aggregate backfill combinations investigated in this study. In each figure, the curves represent the pullout force-displacement relationships for a given aggregate backfill under different normal stresses.

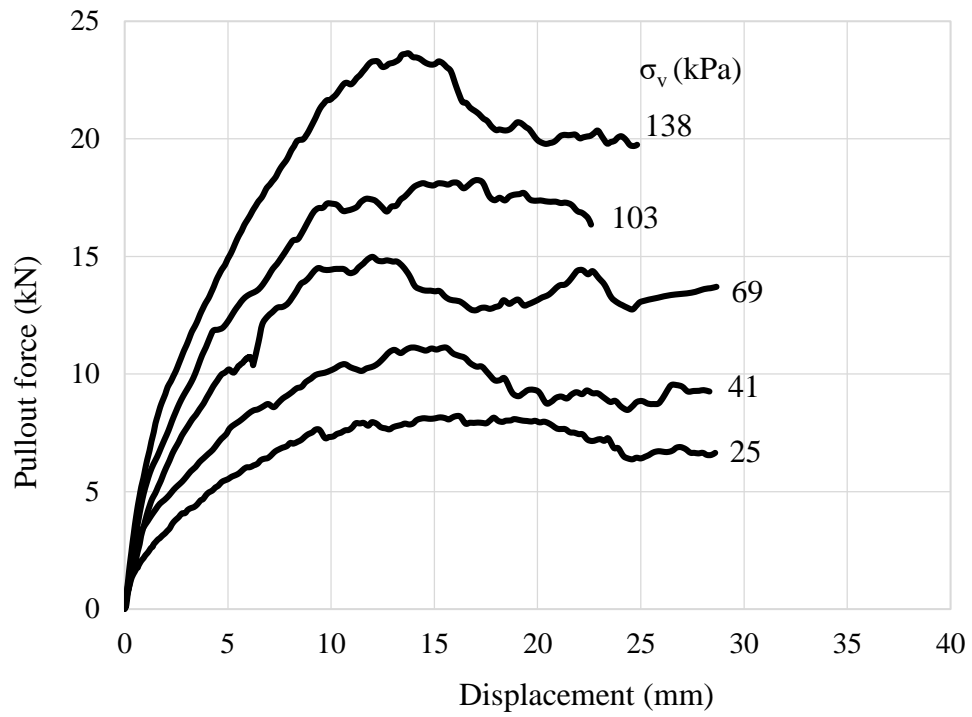


**Figure 5.4 Pullout force versus displacement curve for aggregate with  $C_u=1.4$**

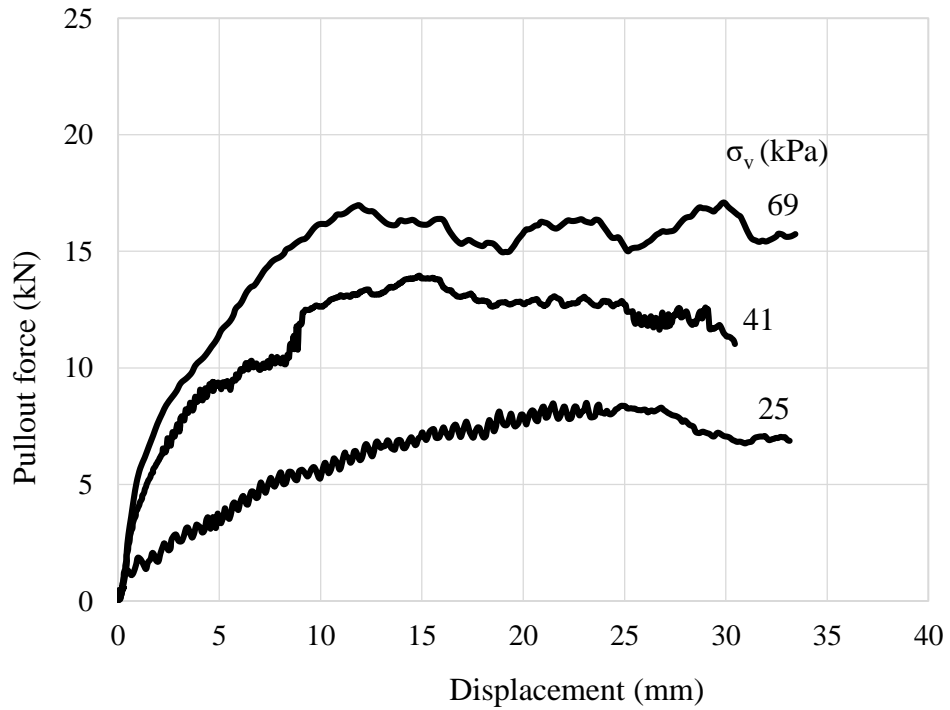


**Figure 5.5 Pullout force versus displacement curve for aggregate with  $C_u=2$**

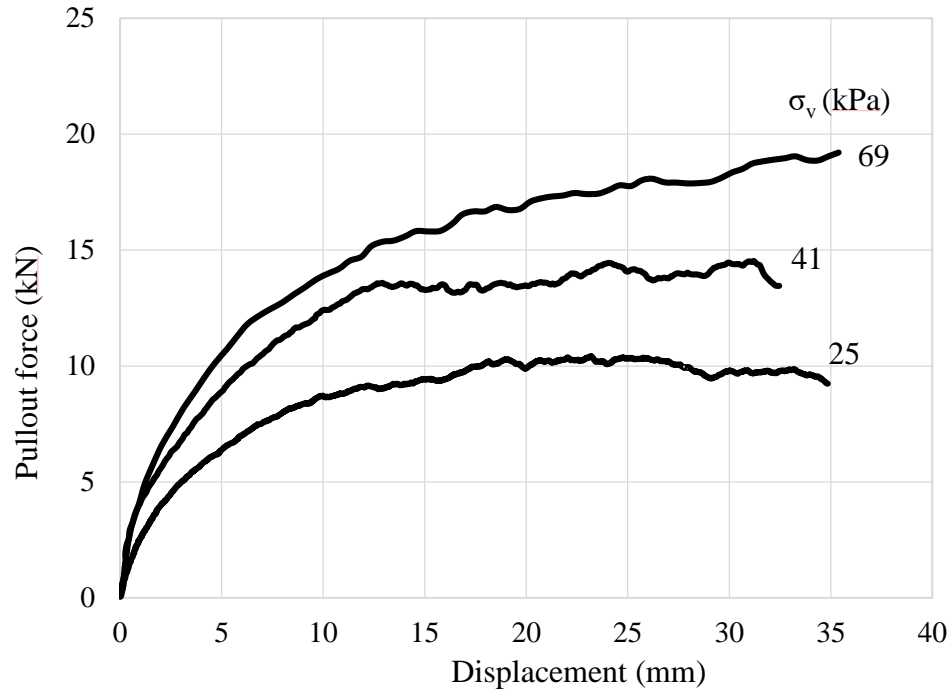


**Figure 5.6 Pullout force versus displacement curve for aggregate with Cu=3**

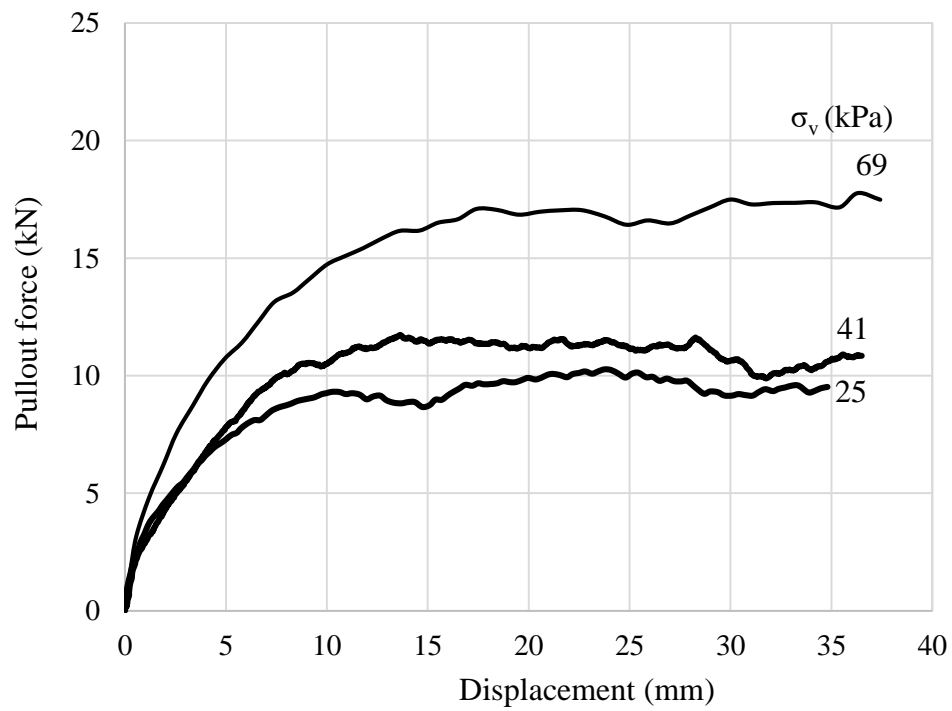


**Figure 5.7 Pullout force versus displacement curve for aggregate with Cu=4**



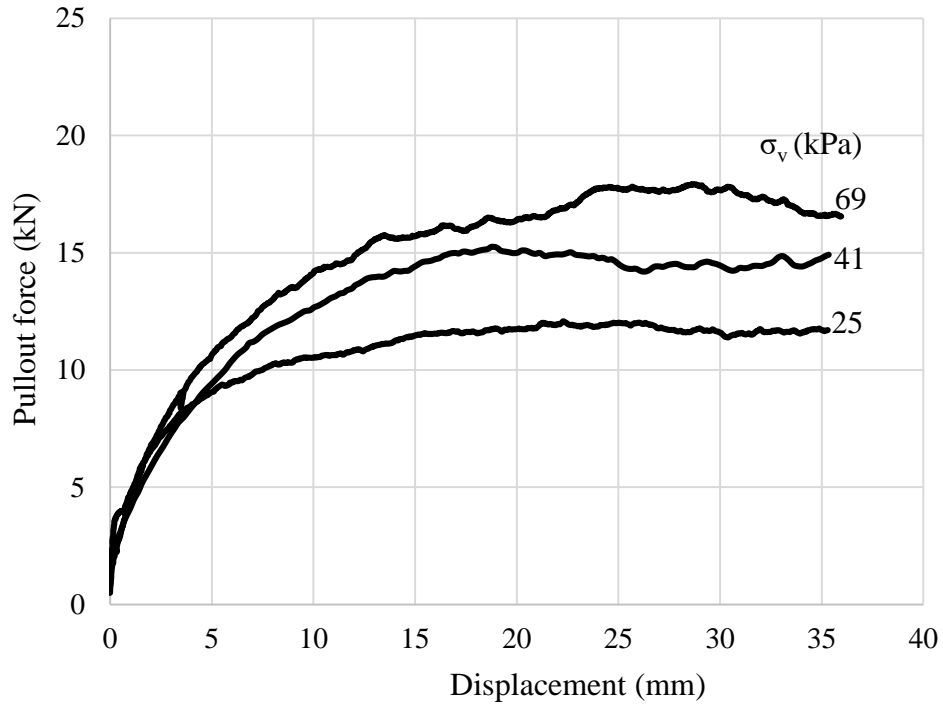


**Figure 5.8 Pullout force versus displacement curve for aggregate with Cu=6**

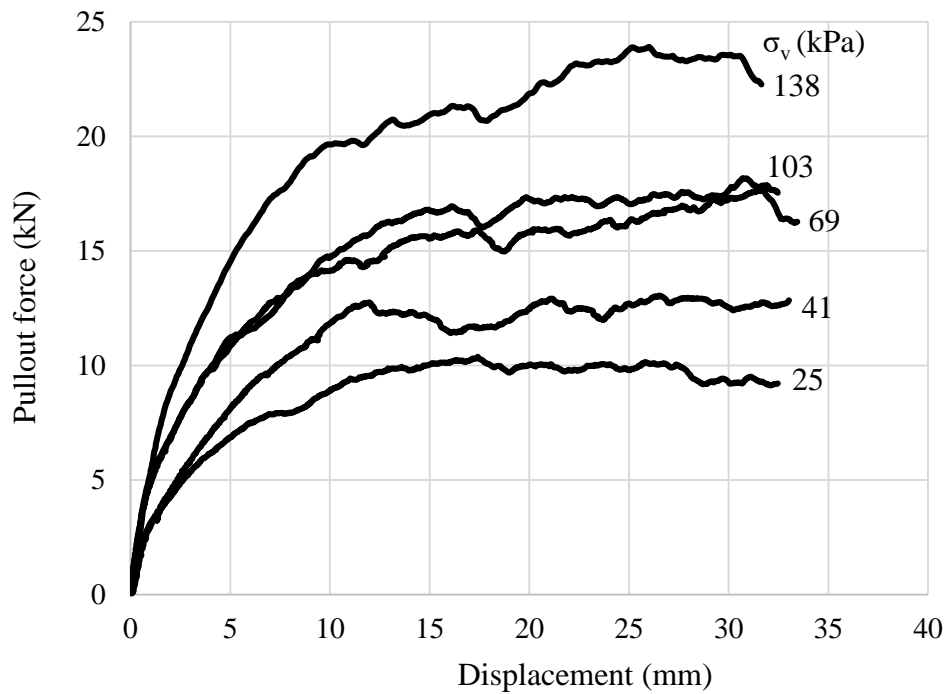


**Figure 5.9 Pullout force versus displacement curve for aggregate with Cu=14**

The pullout force-displacement curves presented above had similar trends for a specific applied normal stress. Moreover, for a particular type of aggregate backfill, the pullout resistance increased with the increase in the normal stress. In most of the tests, the displacement at the peak pullout resistance for a given aggregate backfill was insignificantly affected by the normal stress. However, most of the aggregates with lower uniformity coefficient mobilized to peak resistance at smaller displacements than aggregates with higher uniformity coefficient.

FHWA (2001) suggested that for inextensible reinforcements the ultimate pullout resistance should be selected as the pullout force corresponding to the front displacement of 20 mm unless the peak resistance occurs first. The need for this allowable displacement criterion is to limit the magnitude of earth structure deformations. The ultimate pullout resistance estimated based on the FHWA guideline was used to calculate the pullout resistance factor,  $F^*$ , for the all tests in this study.

Figure 5.10 shows the relationship between the applied normal stress and the measured ultimate pullout resistance. It is shown that the ultimate pullout resistance increased with the confining stress. More specifically, for Type 1 ( $C_u=1.4$ ), the relationships were found to be almost linear.

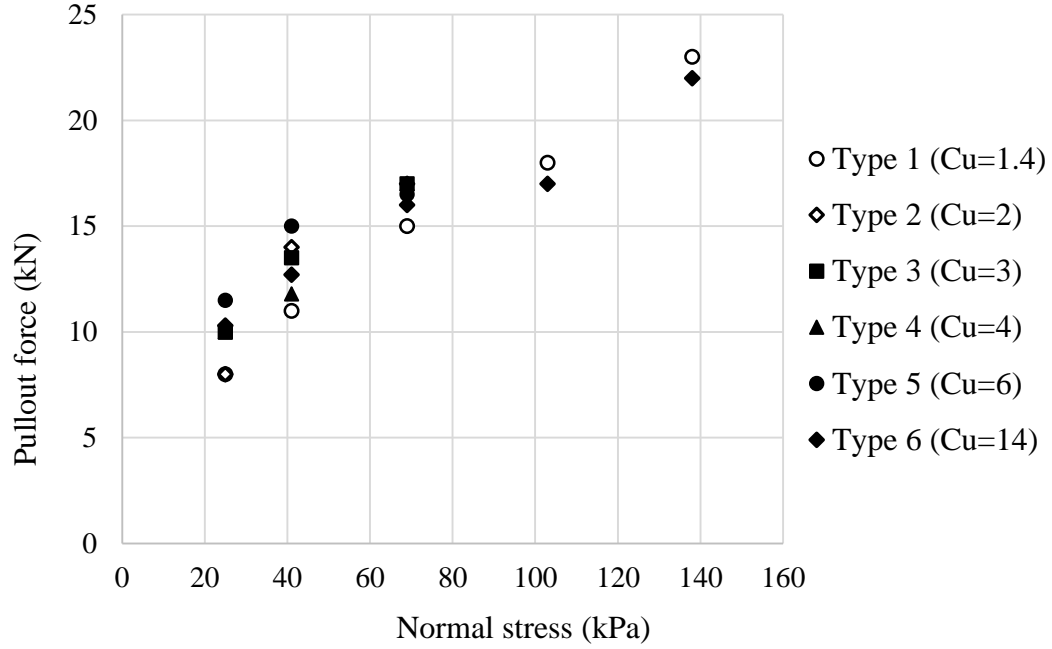


**Figure 5.10 Normal stress-pullout force curves**

#### **5.4 Pullout Resistance Factor, $F^*$**

The ultimate pullout resistance of a reinforcement can be evaluated using a pullout resistance factor,  $F^*$ , which combines the overall soil-reinforcement interaction. In this study, the pullout resistance factors,  $F^*$ , for ribbed steel strip reinforcements were calculated from the test results using Equation 5.1. The parameters used to estimate  $F^*$  values from this study are summarized in APPENDIX C of this thesis.

$$F^* = \frac{P}{\sigma_v L_e b C \alpha} \quad \text{Equation 5.1}$$

where  $F^*$  = pullout resistance factor,  $P$  = ultimate pullout resistance,  $\sigma_v$  = normal stress at the reinforcement level,  $L_e$  = effective length of reinforcement in the resisting zone,  $b$  = width of strip reinforcement,  $\alpha$  = scale effect correction factor (for steel reinforcement,  $\alpha$

=1),  $C$  = overall reinforcement surface area geometry factor based on the gross perimeter of the reinforcement (equal to 2 for strip, grid and sheet-type reinforcements).

In a field project, the normal stress at a certain depth can be estimated as the unit weight of the backfill multiplied by the depth. To analyze the laboratory pullout test results, the corresponding depth of backfill was estimated as the normal stress divided by the unit weight of the backfill. Figure 5.11 presents the  $F^*$  values obtained from the pullout tests in this study versus the depth of backfill, as compared with the AASHTO reference line for ribbed steel strip reinforcement. The AASHTO reference line is plotted using Equations 2.6 and 2.7 for  $C_u = 4$  and internal friction angle of  $34^\circ$ . AASHTO (2012) suggested that the reference line can only be used for backfill materials with the uniformity coefficient,  $C_u \geq 4$ . However, Figure 5.11 shows that all the data points from the pullout tests in this study lie considerably far to the right of the AASHTO reference line. In other words, the AASHTO default  $F^*$  values are conservative as compared with the test data, even for the aggregates with the uniformity coefficient,  $C_u < 4$ . It should be pointed out that the test results in Figure 5.11 had some overlapped data points, which indicate the same  $F^*$  values for different aggregate backfills at the same normal stress.

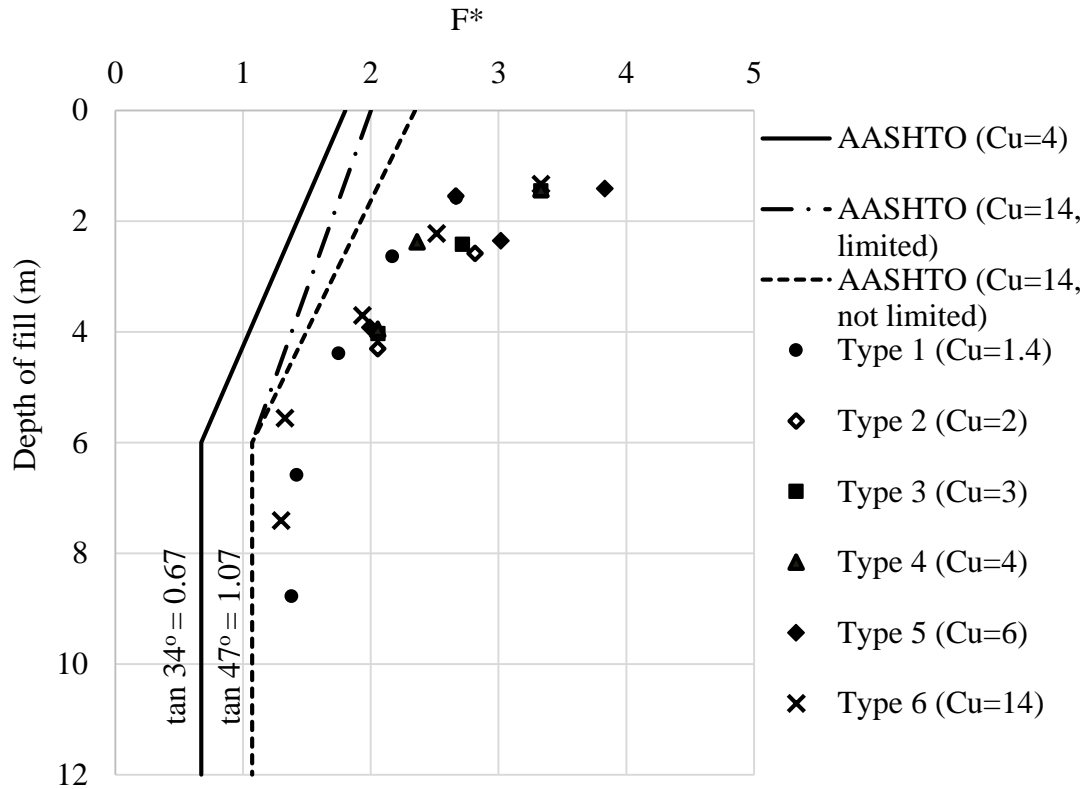


**Figure 5.11  $F^*$  values for ribbed steel strip reinforcement in aggregate backfills**

For all types of aggregate backfills used in this study, the  $F^*$  values decreased with the increase in the depth of fill. This trend indicates that the pullout resistance factor of ribbed strip reinforcement depends on the overburden stress. This result is consistent with the AASHTO reference line. Even though the test results have some variations, there is a general implication that the aggregate with a higher uniformity coefficient had higher  $F^*$  factors than that with a lower uniformity coefficient. The difference in the  $F^*$  factor between the aggregates with different uniformity coefficients became less when the depth of fill got larger. The  $F^*$  factors for different aggregates at the depth of fill about 4 m (i.e. 69 kPa) were almost the same. As shown in Figure 5.11, the  $F^*$  results also lie to the right

of the line plotted based on Equations 2.6 and 2.7 for the highest  $C_u=14$  and average internal friction angle of  $47^\circ$  used in this study.

The coefficient of interface,  $C_i$ , for each backfill-reinforcement combination was calculated based on Equation 5.2. As shown in Figure 5.12, the relationship is linear for all aggregates.

$$C_i = \frac{F^*}{\tan \phi} \quad \text{Equation 5.2}$$

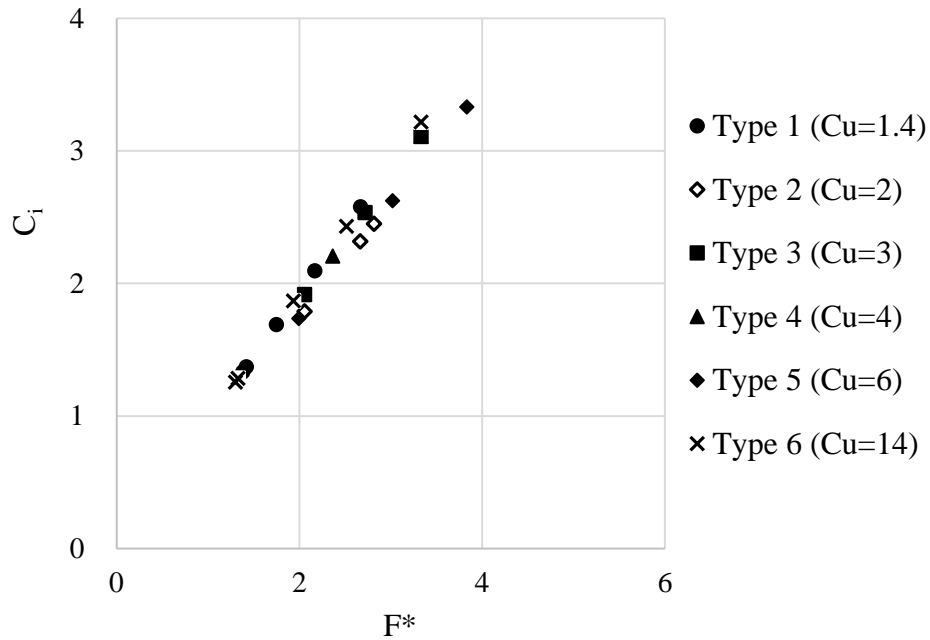


**Figure 5.12  $F^*$  values versus coefficient of interface for each aggregate backfill**

## **CHAPTER 6 CONCLUSIONS AND RECOMMENDATIONS**

The objective of this study was to verify the AASHTO formula (AASHTO, 2012) or develop new one that is applicable for estimating pullout resistance of steel strip reinforcement embedded in uniform aggregates available in Kansas quarries. To achieve this objective, 22 large-scale pullout tests were conducted to investigate the effect of aggregate uniformity on the pullout resistance of ribbed steel strip reinforcement in six aggregates with the uniformity coefficients ranging from 1.4 to 14. The following conclusions and recommendations can be made based on the experimental study.

### **6.1 Conclusions**

1. Pullout test results showed that ribbed steel strip reinforcement in all types of aggregates had similar overall trends of pullout force versus displacement curves. However, there is a general implication that aggregates with a higher uniformity coefficient had higher resistance than that with a lower uniformity coefficient. This can be associated to higher density or soil dilation phenomenon in aggregates of higher  $C_u$ .
2. At a lower normal stress (i.e. 25 kPa), the steel reinforcement in the aggregate with the lowest uniformity coefficients ( $C_u = 1.4$  and 2) had the lowest pullout resistance. At a higher normal stress (i.e. 69 kPa), however, all aggregates resulted in nearly the same pullout resistance. In other words, the aggregate uniformity had more effect on the pullout resistance at a lower normal stress than that at a higher normal stress

because soil dilation is minimized under higher confinement with an increase of the overburden depth.

3. The test results showed that the ultimate pullout resistance for ribbed steel strip reinforcement increased with the overburden depth whereas the pullout resistance factor,  $F^*$ , decreased with depth.

4. The measured pullout resistance factors for all reinforcement-backfill combinations regardless of the uniformity are higher than the default  $F^*$  values for ribbed strip reinforcement recommended by AASHTO (2012). This comparison indicates that the  $F^*$  values recommended by AASHTO (2012) are conservative for ribbed steel strip reinforcement in crushed stone aggregates. The formula suggested by AASHTO (2012) can be used to conservatively estimate the  $F^*$  value (not limited by 2) with the uniformity coefficient as low as 1.4.

## **6.2 Recommendations**

1. Based on the test results in this study, the aggregate uniformity had some effects on the calculated  $F^*$  value at a lower normal stress but its effect became minimal at a higher normal stress. Since the AASHTO default  $F^*$  line is conservative for aggregates with the uniformity coefficient of  $1.4 \leq C_u < 4$  or  $C_u \geq 4$ , it can be used for the aggregates with the uniformity coefficient of  $C_u \geq 1.4$ , provided the aggregate satisfies the standard backfill gradation requirements.

2. The conclusions obtained from this study are based on ribbed steel reinforcement in aggregate backfill. Further studies are needed to verify these conclusions for other type of steel reinforcement and backfill.



## REFERENCES

- AASHTO (2010). AASHTO LRFD Bridge Construction Specifications, 3rd Edition, Section 7: Earth Retaining Systems. American Association of State Highway and Transportation Officials, Washington D.C.
- AASHTO (2012). *AASHTO LRFD Bridge Design Specifications, 6th Edition, Section 11: Abutments, Piers, and Walls*. American Association of State Highway and Transportation Officials, Washington D.C.
- ASTM Standard D4253 (2000a). *Standard Test Methods for Maximum Index Density and Unit Weight of Soils and Calculation of Relative Density*. Annual Book of ASTM Standards, ASTM International, West Conshohocken, PA.
- ASTM Standard D4254 (2000b). *Standard Test Methods for Minimum Index Density and Unit Weight of Soils Using a Vibratory Table*. Annual Book of ASTM Standards, ASTM International, West Conshohocken, PA.
- ASTM Standard D6706 (2001). *Standard Test Method for Measuring Geosynthetic Pullout Resistance in Soil*. Annual Book of ASTM Standards, ASTM International, West Conshohocken, PA.
- ASTM Standard D422 (2007). *Standard Test Method for Particle Size Analysis of Soils*. Annual Book of ASTM Standards, ASTM International, West Conshohocken, PA.
- ASTM Standard D7181 (2011). *Standard Test Method for Consolidated Drained Triaxial Compression Test for Soils*. Annual Book of ASTM Standards, ASTM International, West Conshohocken, PA.
- ASTM Standard D698-12e1 (2012). *Standard Test Methods for Laboratory Compaction Characteristics of Soil Using Standard Effort*. . Annual Book of ASTM Standards, ASTM International, West Conshohocken, PA.
- Chang, J. C., Hannon, J. B., and Forsyth, R. A. (1977). "Pull Resistance and Interaction of Earthwork Reinforcement and Soil." Transportation Research Board 56th Annual Meeting 10.

- FHWA (2001). *Mechanically Stabilized Earth Walls and Reinforced Soil Slopes Design and Construction Guidelines*. Federal Highway Administration (FHWA), FHWA-NHI-00-043, Washington, D.C.
- Kansas Department of Transportation (KDOT) (2007). Special Provision to the Standard Specifications, Edition 2007, Section 1107, Aggregates for Backfill.
- Lawson, W., Jayawickrama, P., Wood, T., and Surles, J. (2013a). "Pullout Resistance of Mechanically Stabilized Earth Reinforcements in Backfills Typically Used In Texas." TxDOT Research Report, FHWA/TX-13/0-6493-1.
- Lawson, W., Jayawickrama, P., Wood, T., and Surles, J. (2013b). "Pullout Resistance Factors for Steel Reinforcements Used in TxDOT MSE Walls." Geo-Congress 2013, ASCE: pp. 44-53.
- Lee H.S. and Bobet A. (2005). "Laboratory Evaluation of Pullout Capacity of Reinforced Silty Sands in Drained and Undrained Conditions." *Geotechnical Testing Journal*, Volume 28, No.4, pp. 370-379.
- Peterson L. M. (1980). "Pullout Resistance of Welded Wire Mesh Embedded in Soil." M.S. Thesis, Utah State University, Logan, Utah.
- Rathje, E. M., Rauch, A. F., Trejo, D., Folliard, K. J., Viyanant, C., Esfellar, M., and Ogalla, M. (2006). "Evaluation of Crushed Concrete and Recycled Asphalt Pavement as Backfill for Mechanically Stabilized Earth Walls." FHWA/TX-06/0-4177-3.
- Reinforced Earth Company website: <http://www.reinforcedearth.com/sites/default/files/File/Reinforced%20Earth%20Brochure.pdf>.
- The Reinforced Earth Company (1995). *Technical Bulletin, MSE-6: Apparent Coefficient of Friction,  $f^*$ , to be Used in the Design of Reinforced Earth Structures*.
- Vidal, H. (1969). "The principle of Reinforced Earth." *Highway Research Record* 282, pp 1-16.

## APPENDIX A

### BACKFILL MATERIAL GRADATION

Table A.1 presents the particle size distributions of the five aggregate backfills used in this experimental study. The FHWA gradation requirement is also included in this table for comparison and verification.

**Table A. 1 Aggregate backfill gradation summary**

Sieve size	Percent passing (%)						
	FHWA	Type 1	Type 2	Type 3	Type 4	Type 5	Type 6
102 mm	100	-	-	-	-	-	-
25 mm	-	100	100	100	100	100	100
19 mm.	-	82.4	82.9	87.4	89.3	92.5	90.1
12.5 mm	-	9.5	18.7	31.2	50.2	65.9	57.8
No. 4	-	0	1.0	7.7	11.8	17.2	21.0
No. 40	0-60	-	0.6	1.8	0.6	0.5	4.6
No. 200	0-15	-	0.4	0.2	0.4	0.4	2.4
C <sub>u</sub>	-	1.4	2	3	4	6	14

## APPENDIX B

### TRIAXIAL TEST RESULTS

Figures B.1 to B.12 show the stress-strain curves and the Mohr's circles for the six types of aggregates at the normal stresses corresponding to 5% strain.

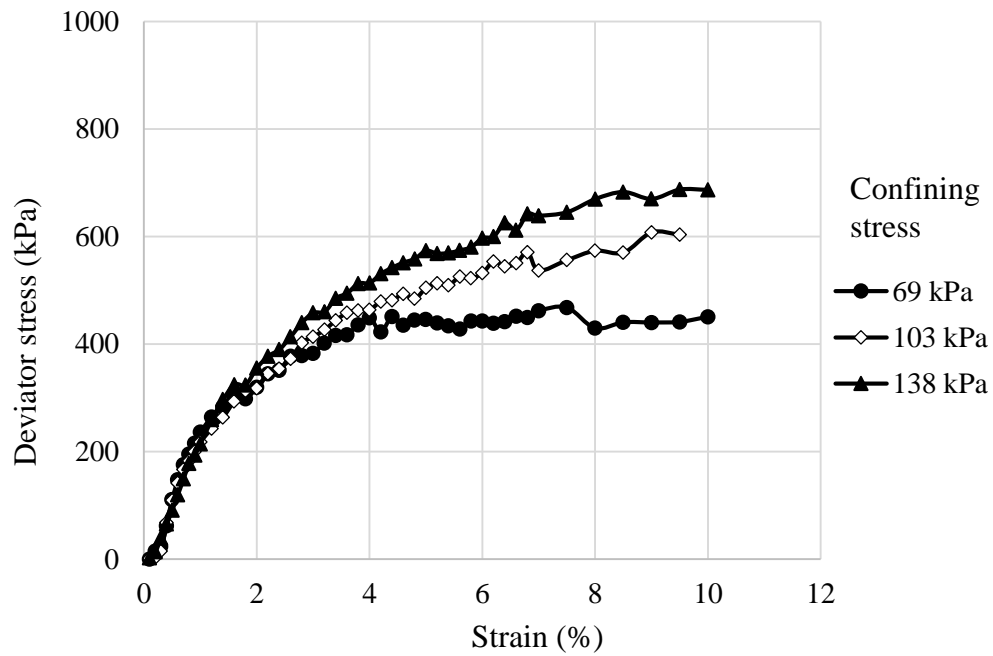
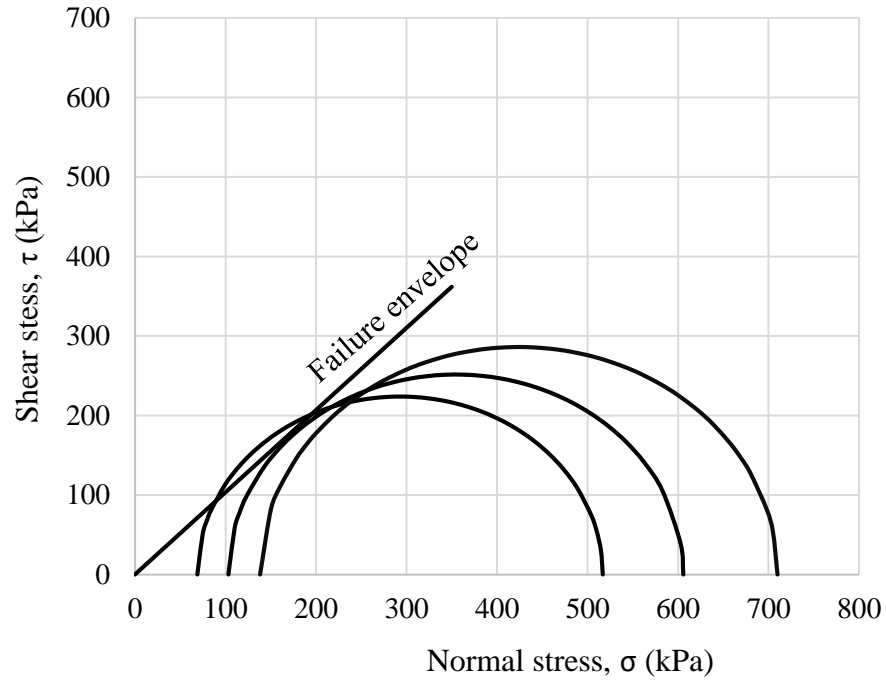
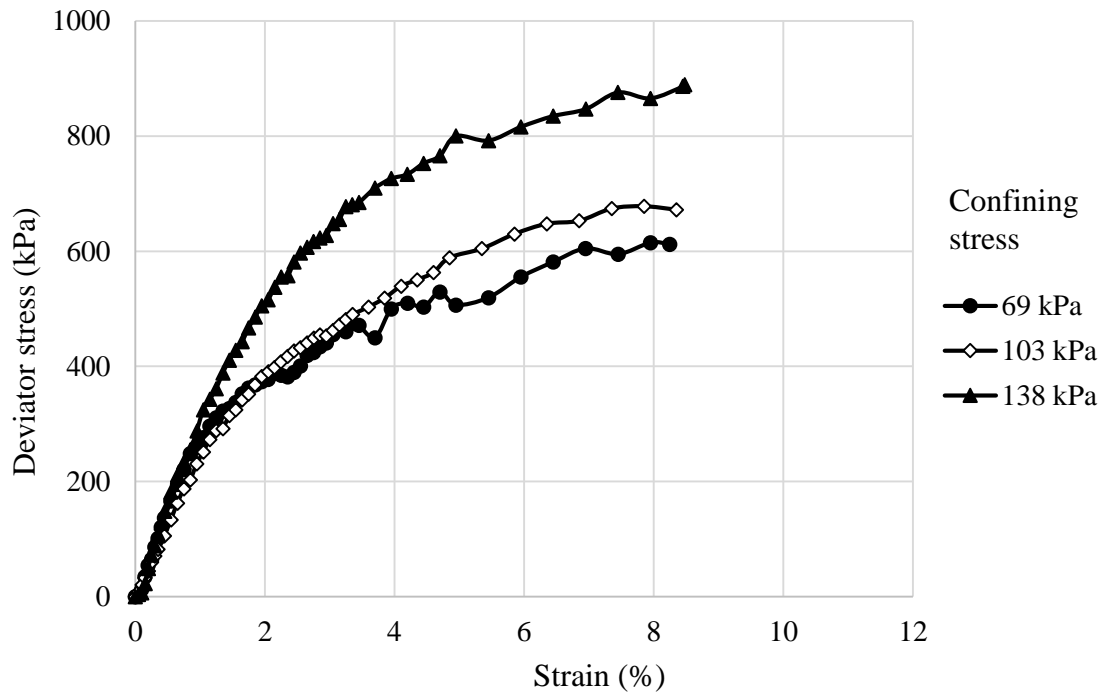


Figure B. 1 Stress-strain curves for Cu=1.4



**Figure B. 2 Mohr circles for  $Cu=1.4$**



**Figure B. 3 Stress-strain curves for  $Cu=2$**

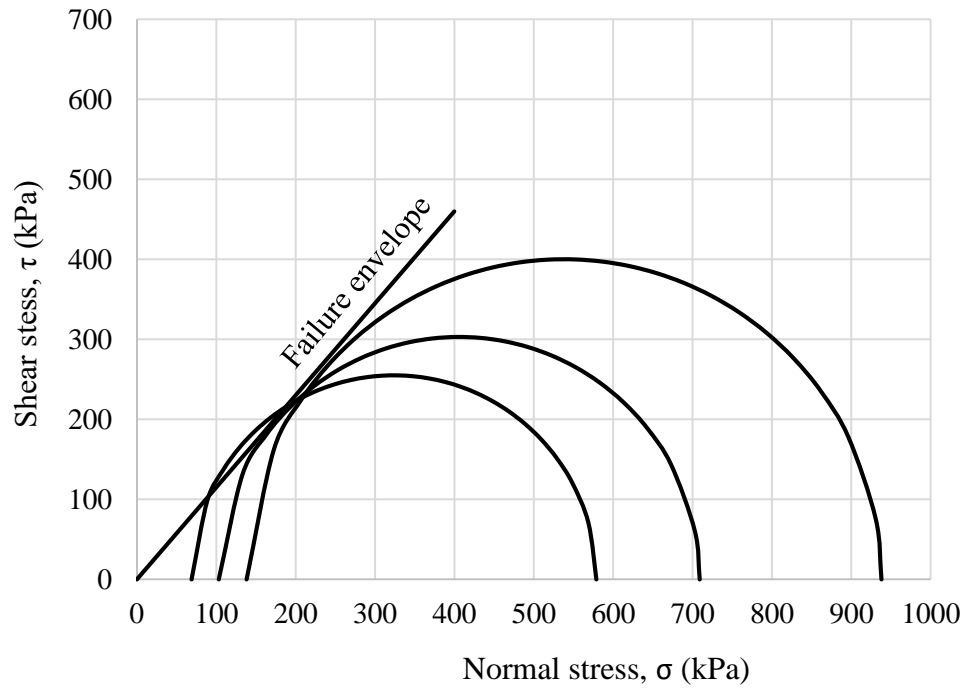


**Figure B. 4 Mohr circles for Cu=2**

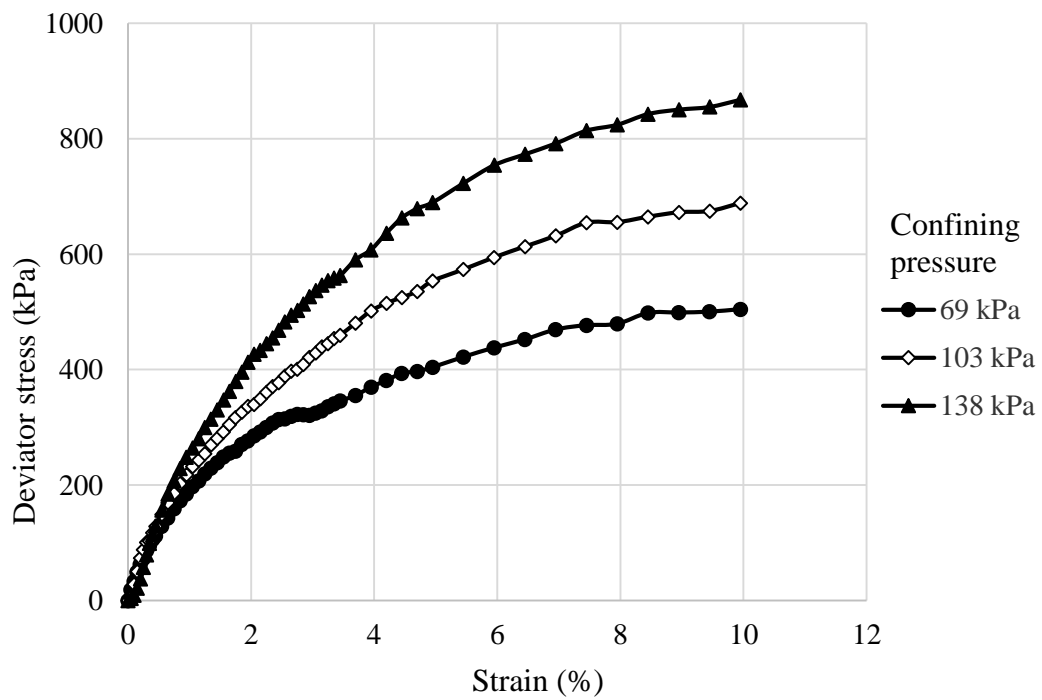


**Figure B. 5 Stress-strain curves for Cu=3**

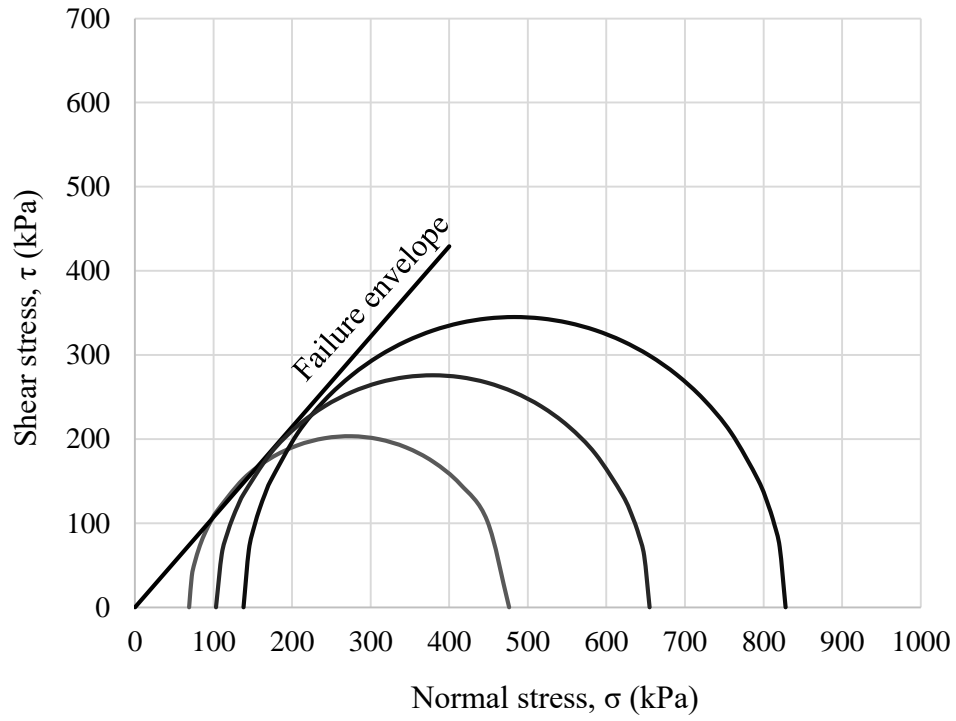


**Figure B. 6 Mohr circles for Cu=3**

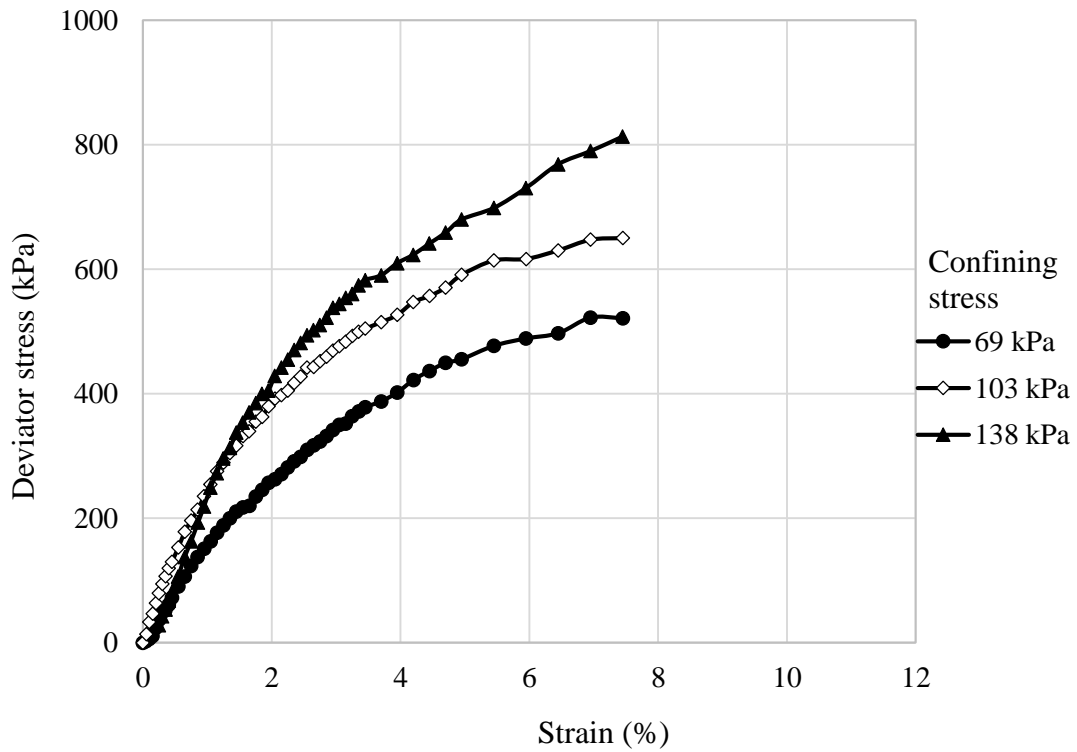


**Figure B. 7 Stress-strain curves for Cu=4**

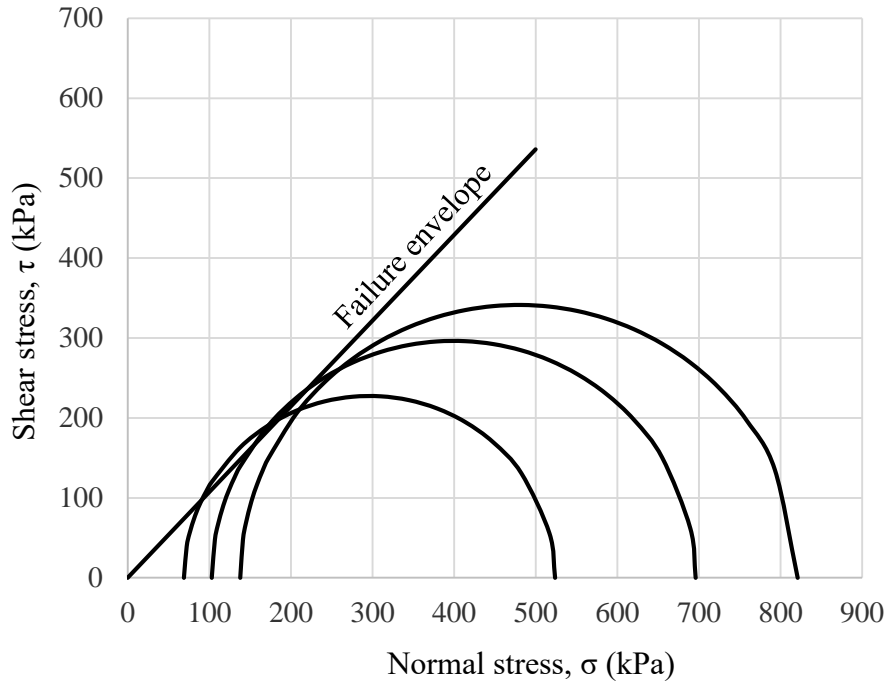


**Figure B. 8 Mohr circles for  $Cu=4$**

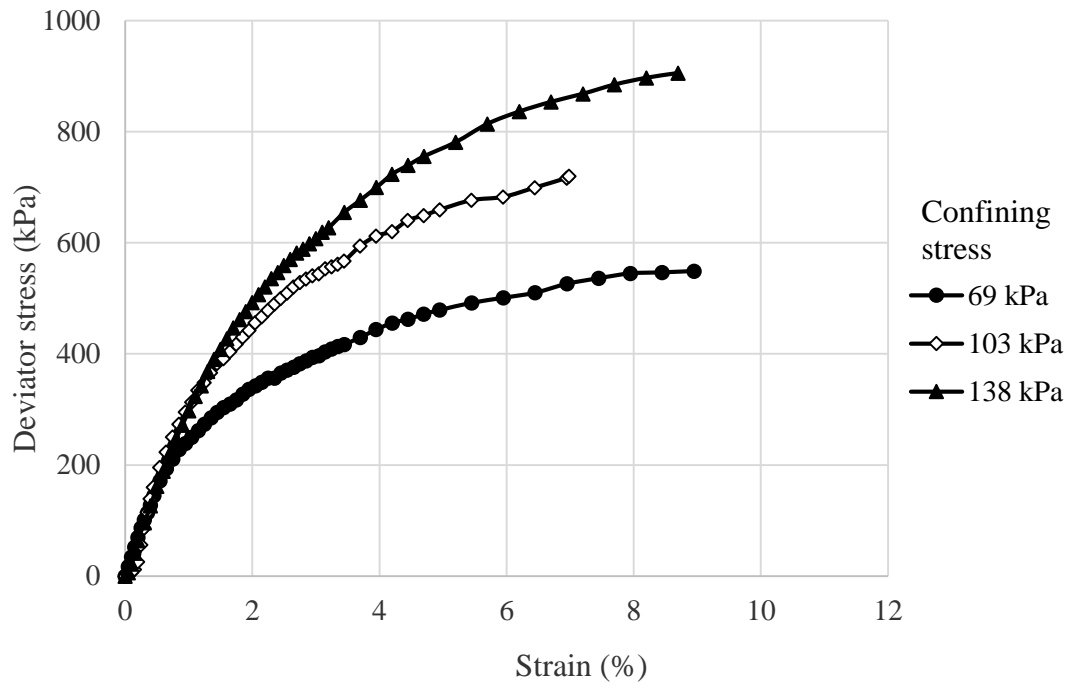


**Figure B. 9 Stress-strain curves for  $Cu=6$**



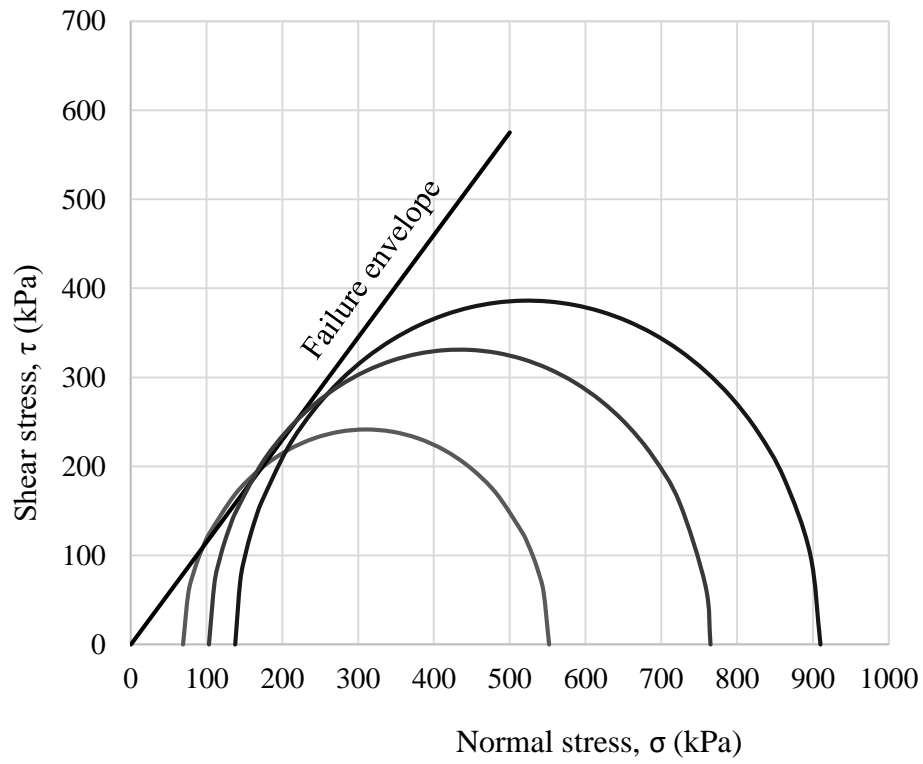


**Figure B. 10 Mohr circles for Cu=6**

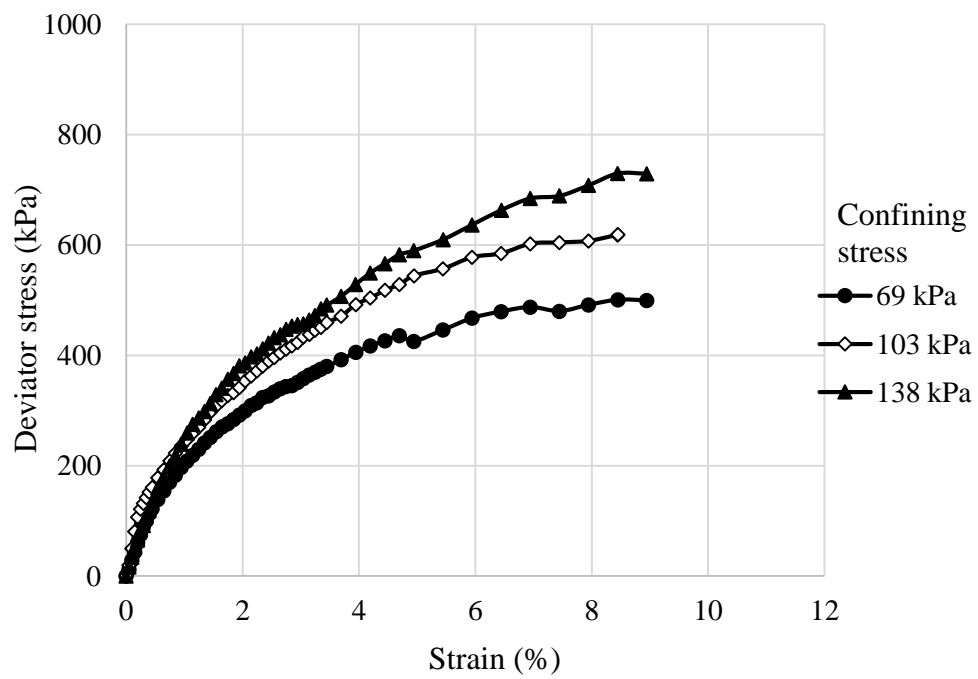


**Figure B. 11 Stress-strain curves for Cu=14**

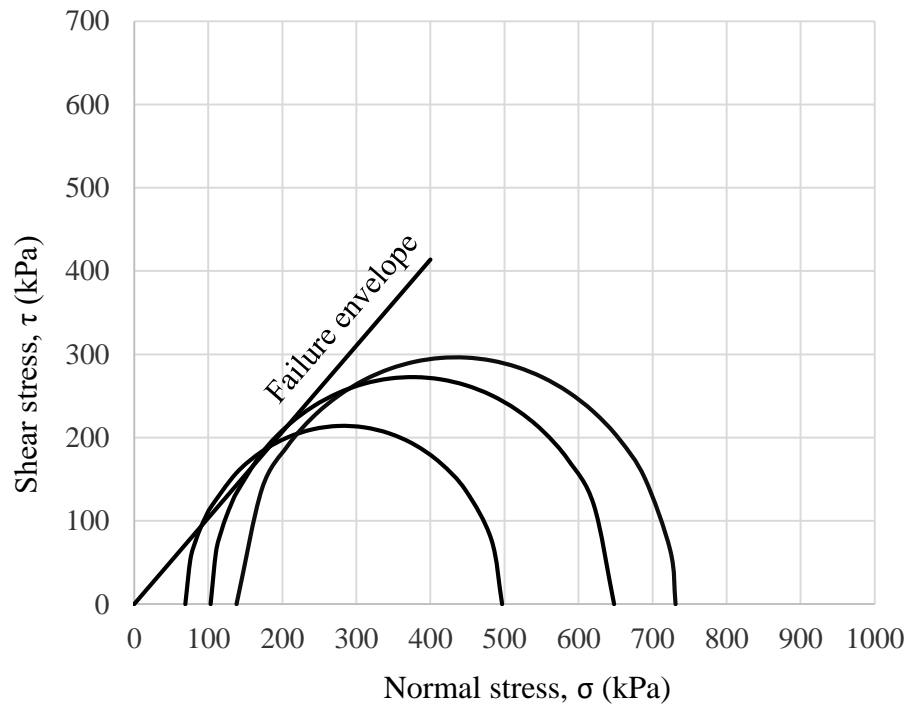


**Figure B. 12 Mohr circles for Cu=14**

## APPENDIX C

### PULLOUT TEST DATA

The test data provided in Table C.1 were used to calculate the pullout resistance factors,  $F^*$ .

**Table C. 1 Summary of pullout test data**

Backfill Type	Uniformity coefficient, $C_u$	Effective length, $L_e$ (mm)	Width, $b$ (mm)	Displacement (mm)	Normal stress, $\sigma_v$ (kPa)	Depth of fill (m)	Pullout force, $P_r$ (kN)	$F^*$
1	1.4	1500	50	15	25	1.6	8	2.67
				15	41	2.6	11	2.17
				12	69	4.4	15	1.75
				15	103	6.6	18	1.42
				13	138	8.8	23	1.38
2	2	1500	50	20	25	1.5	8	2.67
				15	41	2.6	14	2.82
				12	69	4.3	17	2.06
3	3	1500	50	20	25	1.4	10	3.33
				20	41	2.4	13.5	2.72
				20	69	4.0	17	2.06
4	4	1500	50	20	25	1.4	10	3.33
				13	41	2.4	11.8	2.37
				17	69	4.0	17	2.06
5	6	1500	50	20	25	1.4	11.5	3.83
				20	41	2.4	15	3.02
				20	69	3.9	16.5	2.00
6	14	1500	50	17	25	1.3	10.3	3.33
				12	41	2.2	12.7	2.54
				17	69	3.7	16	1.94
				20	103	5.6	17	1.33
				20	138	7.4	22	1.30

The pullout force versus displacement curves for all the tests are provided in Figures C.1 to C.22. In each figure, the two curves correspond to back and front displacement of the strip reinforcement. In some of the tests, the two displacements showed considerable differences (especially at the beginning of the test) which is attributed to improper setup or other imperfections.

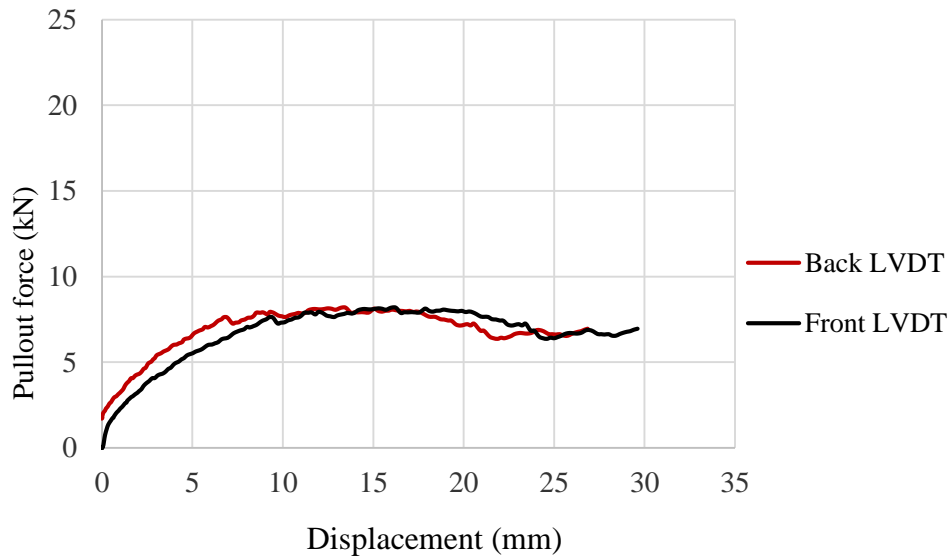


**Figure C. 1 Pullout force-displacement curve for  $C_u=1.4$  at normal stress of 25 kPa**

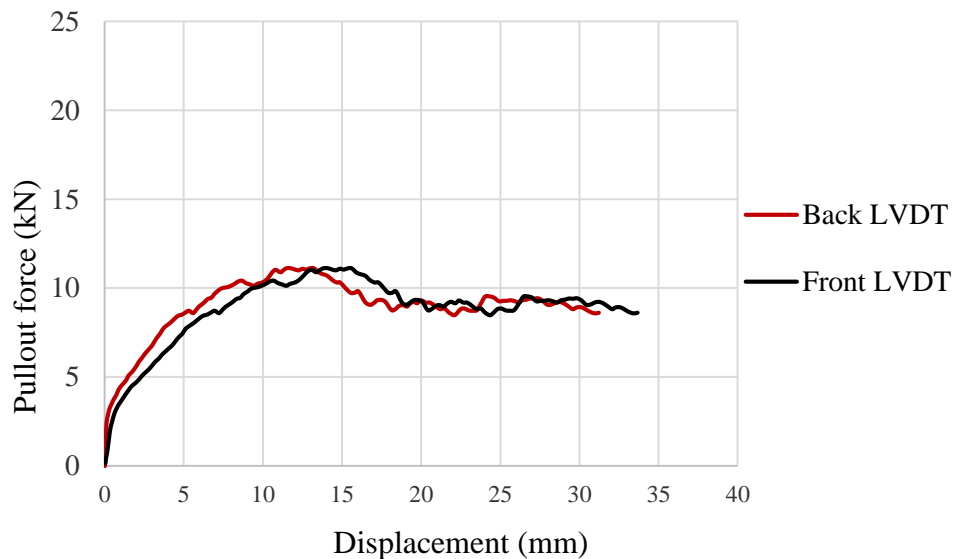


**Figure C. 2 Pullout force-displacement curve for  $C_u=1.4$  at normal stress of 41 kPa**

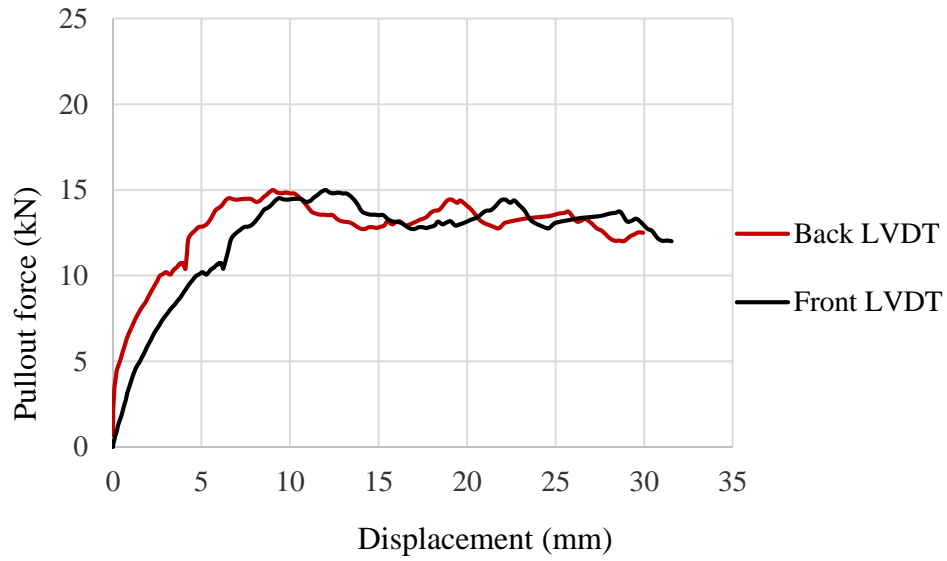


**Figure C. 3 Pullout force-displacement curve for  $Cu=1.4$  at normal stress of 69 kPa**

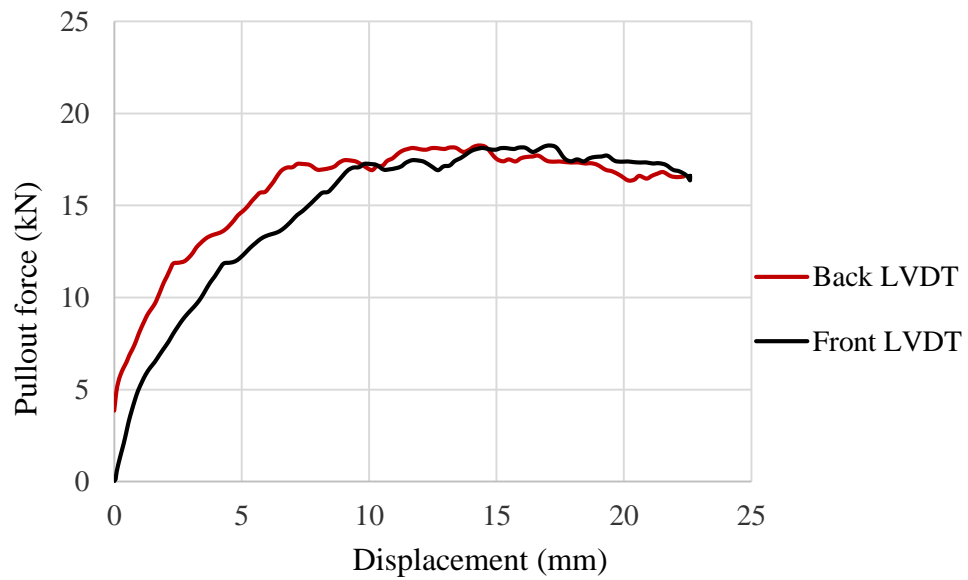


**Figure C. 4 Pullout force-displacement curve for  $Cu=1.4$  at normal stress of 103 kPa**

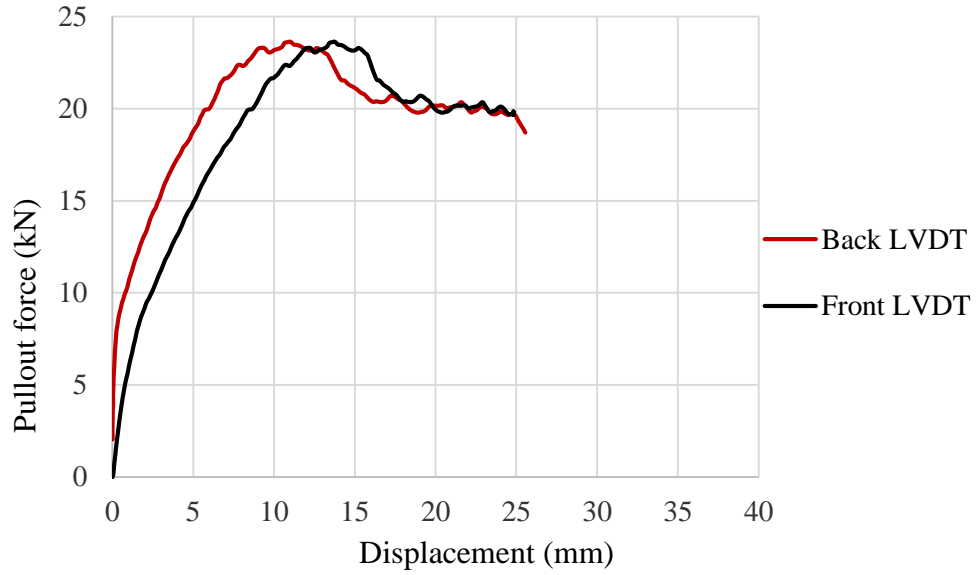


**Figure C. 5 Pullout force-displacement curve for  $Cu=1.4$  at normal stress of 138 kPa**

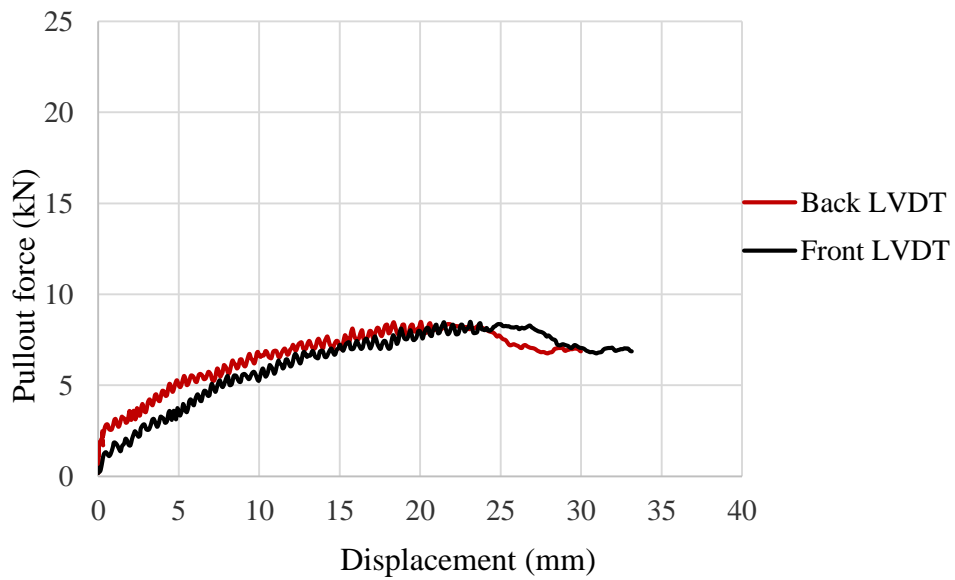


**Figure C. 6 Pullout force-displacement curve for  $Cu=2$  at normal stress of 25 kPa**

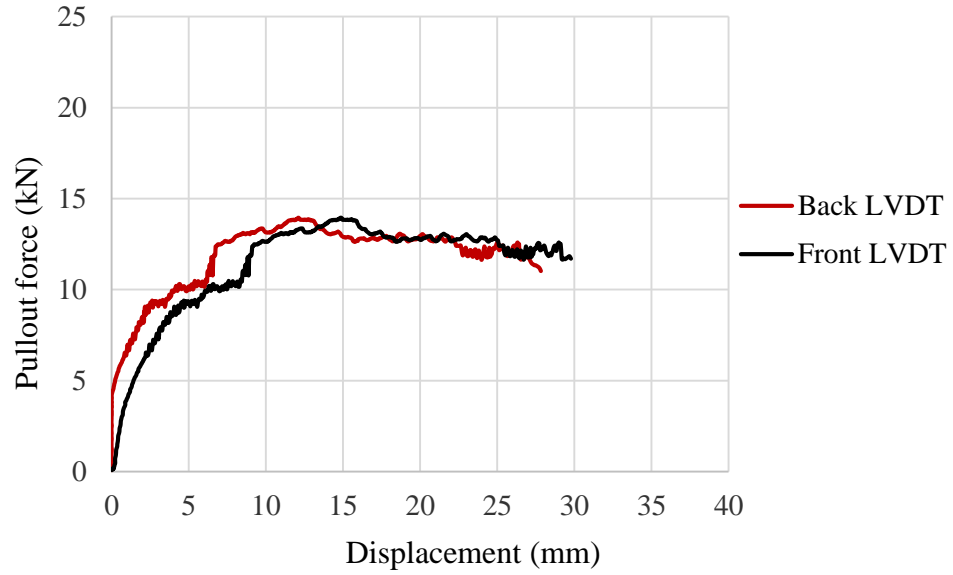


**Figure C. 7 Pullout force-displacement curve for Cu=2 at normal stress of 41 kPa**

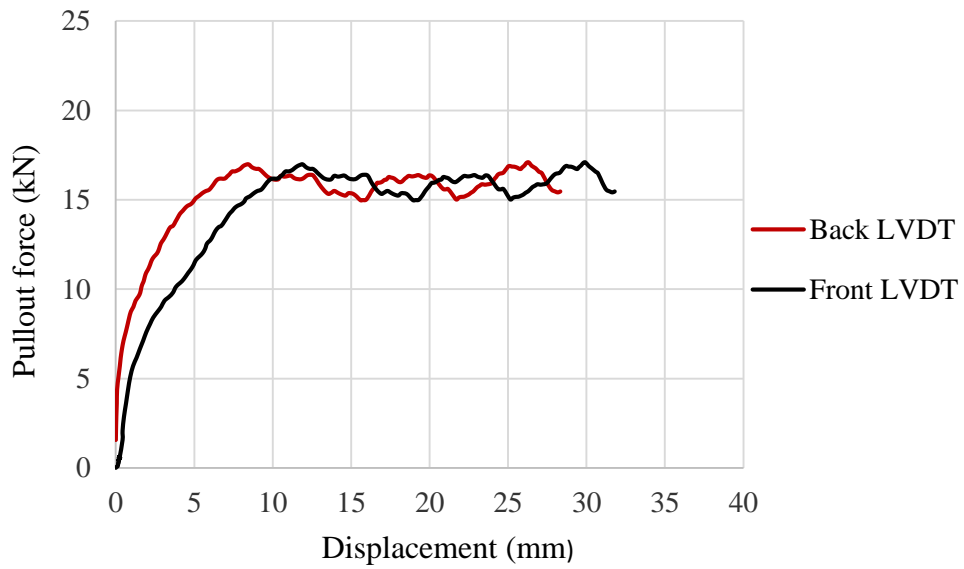


**Figure C. 8 Pullout force-displacement curve for Cu=2 at normal stress of 69 kPa**

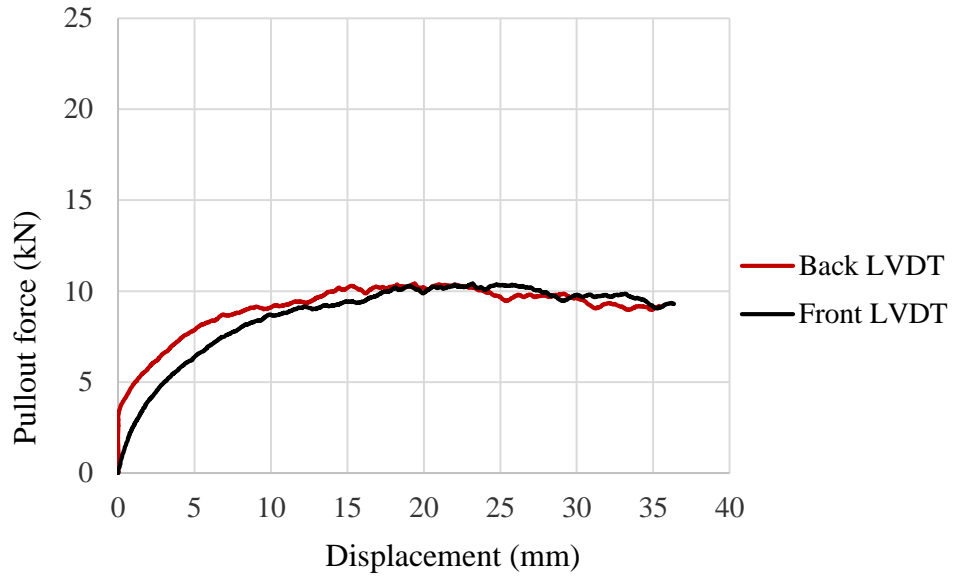


**Figure C. 9 Pullout force-displacement curve for Cu=3 at normal stress of 25 kPa**

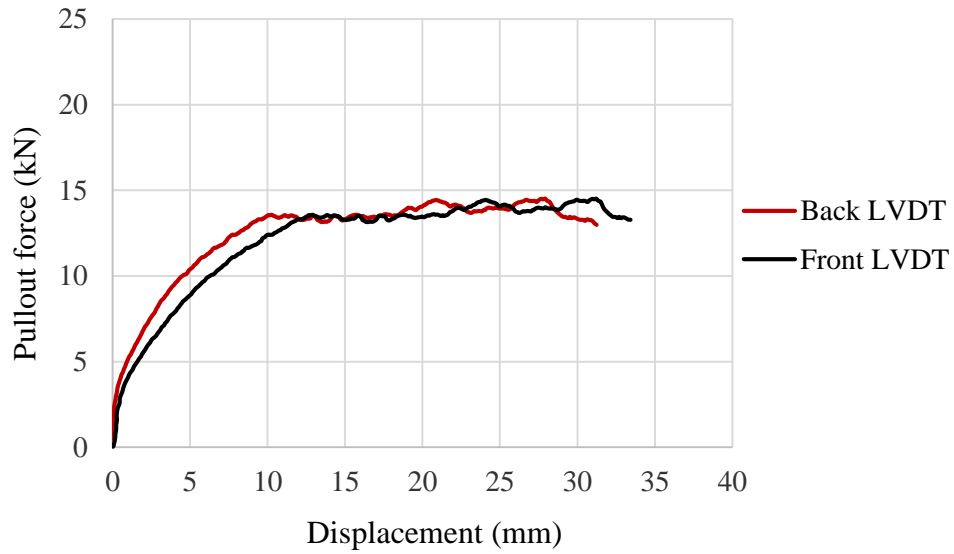


**Figure C. 10 Pullout force-displacement curve for Cu=3 at normal stress of 41 kPa**



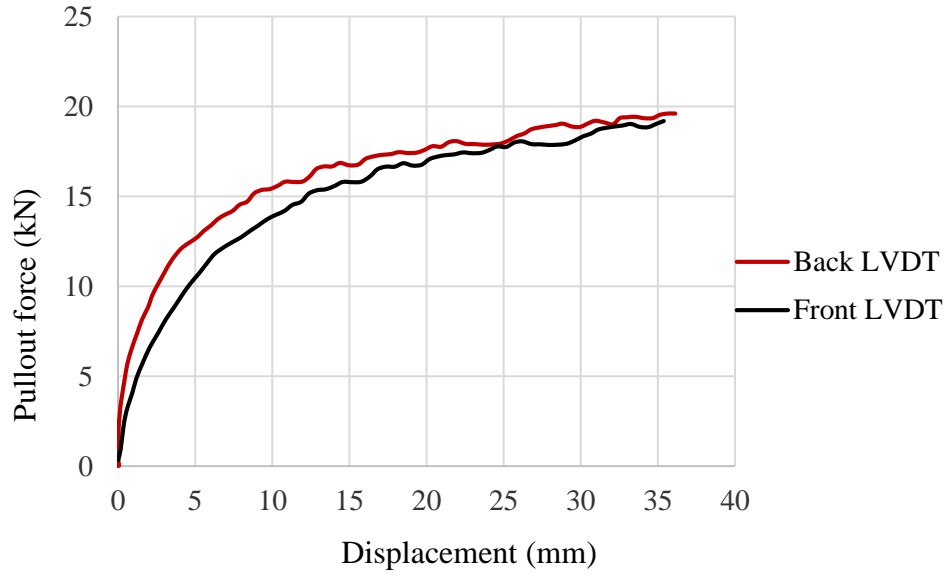


**Figure C. 11 Pullout force-displacement curve for Cu=3 at normal stress of 69 kPa**

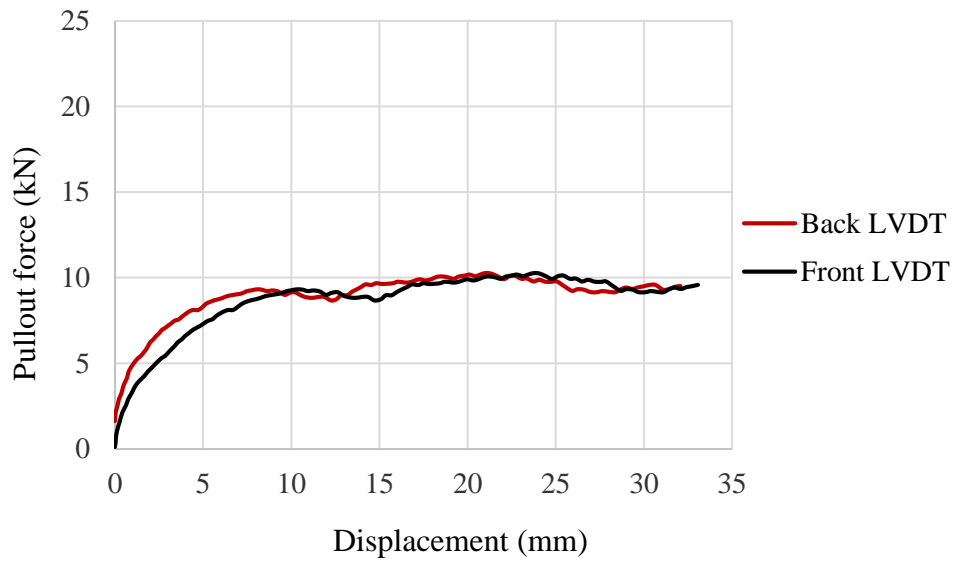


**Figure C. 12 Pullout force-displacement curve for Cu=4 at normal stress of 25 kPa**

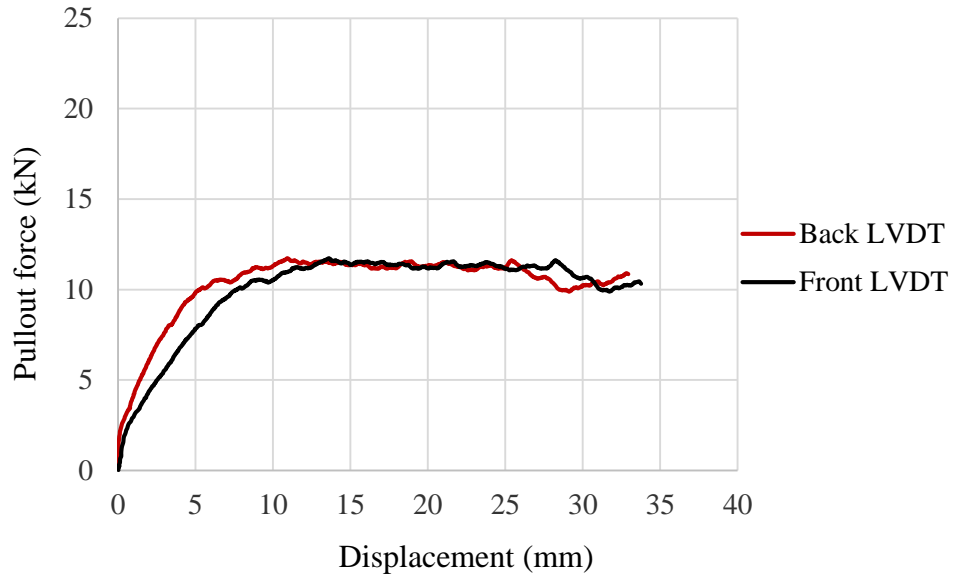


**Figure C. 13 Pullout force-displacement curve for Cu=4 at normal stress of 41 kPa**

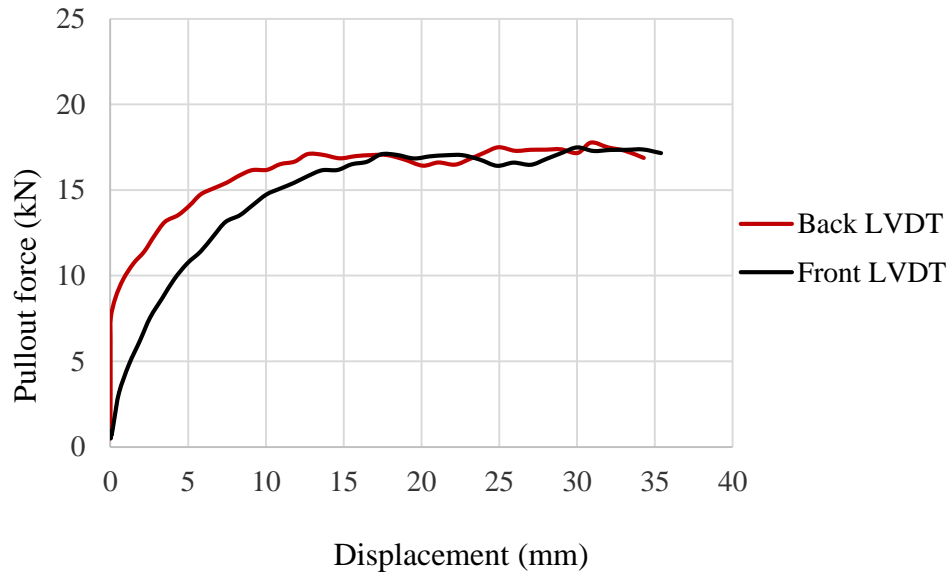


**Figure C. 14 Pullout force-displacement curve for Cu=4 at normal stress of 69 kPa**

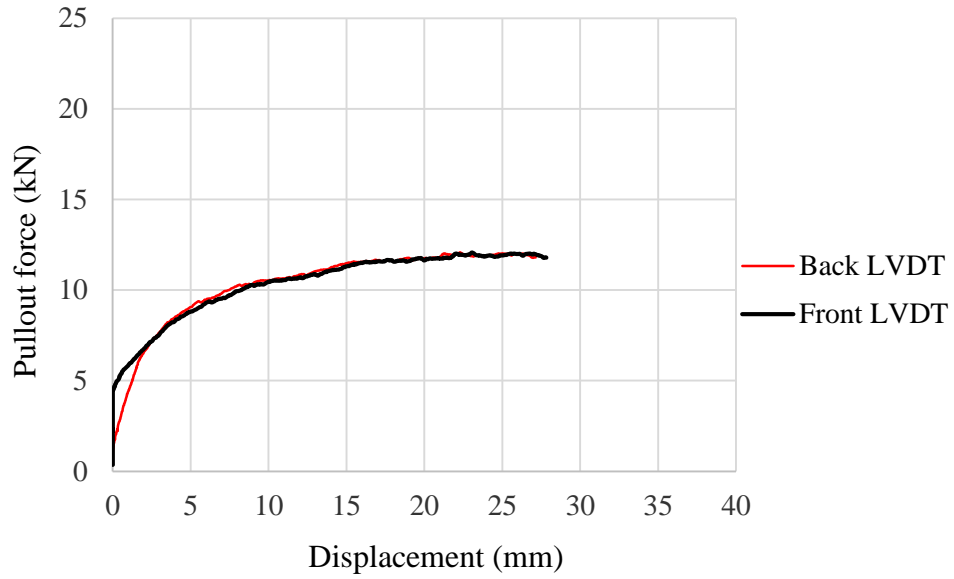


**Figure C. 15 Pullout force-displacement curve for Cu=6 at normal stress of 25 kPa**

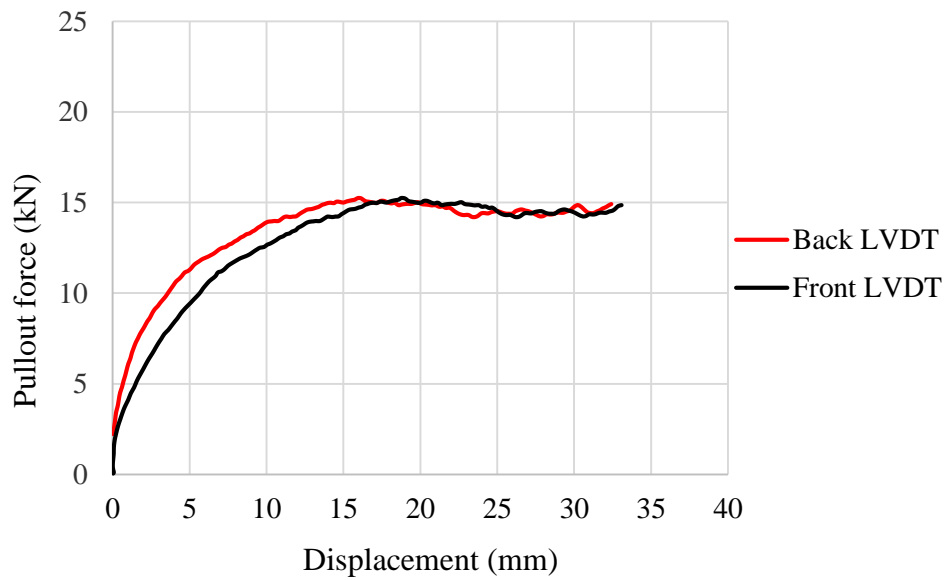


**Figure C. 16 Pullout force-displacement curve for Cu=6 at normal stress of 41 kPa**

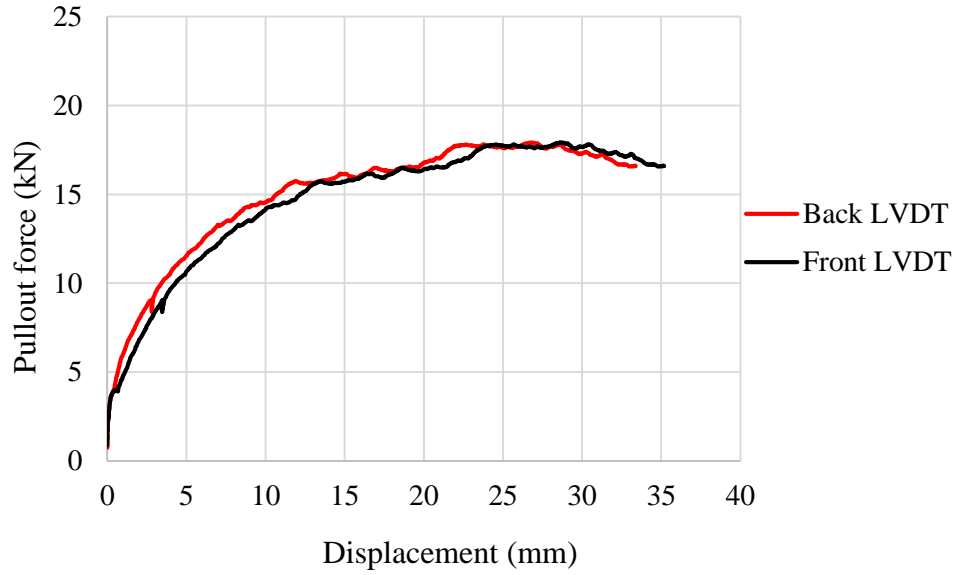


**Figure C. 17 Pullout force-displacement curve for Cu=6 at normal stress of 69 kPa**

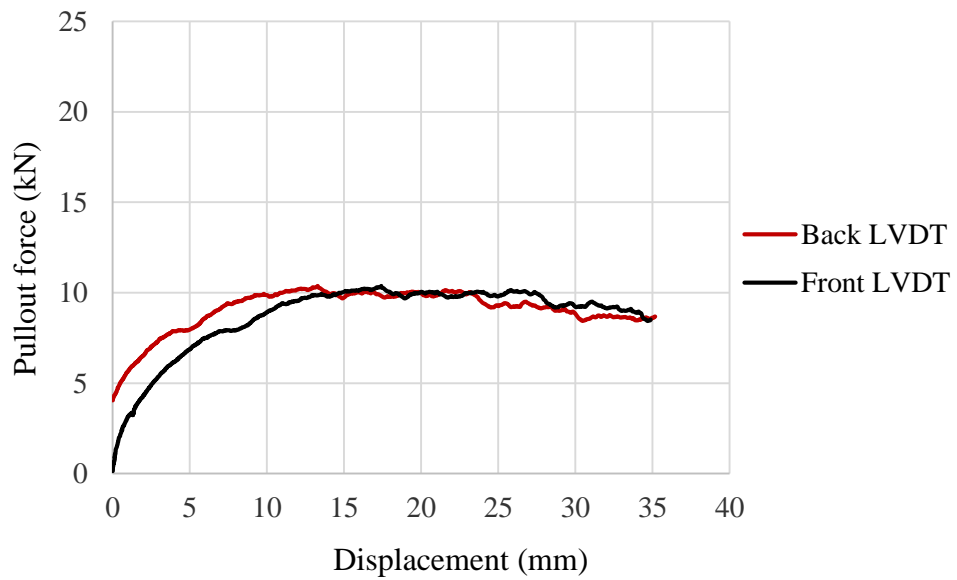


**Figure C. 18 Pullout force-displacement curve for Cu=14 at normal stress of 25 kPa**

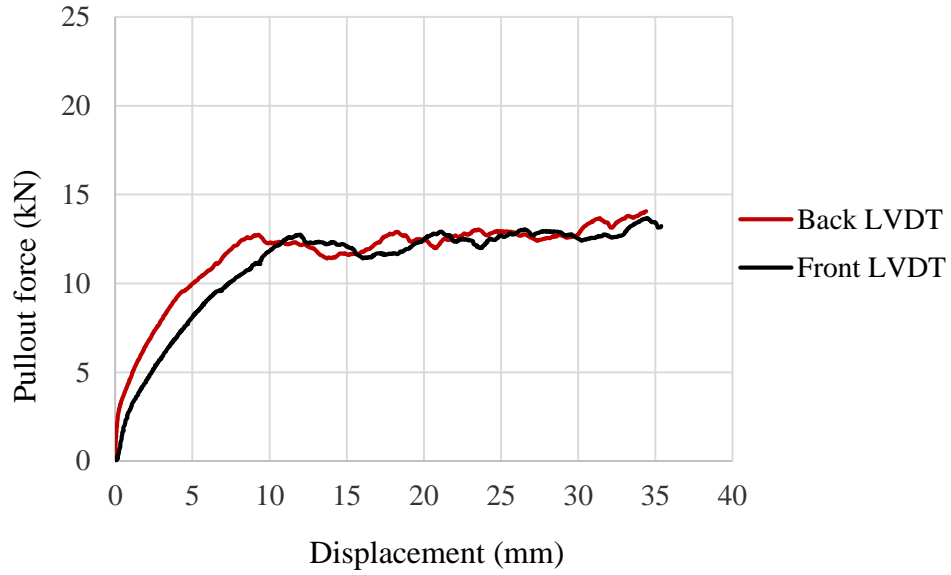


**Figure C. 19 Pullout force-displacement curve for Cu=14 at normal stress of 41 kPa**

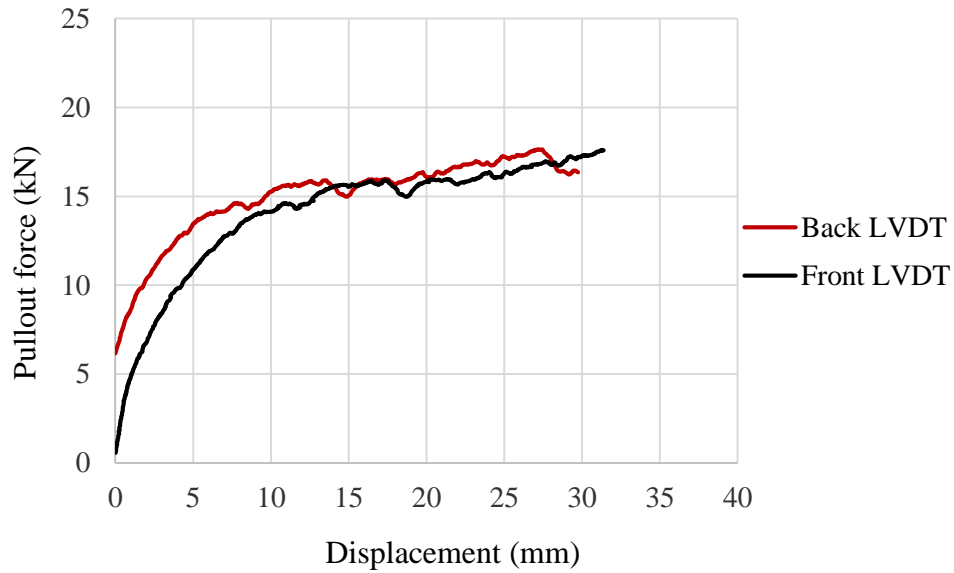


**Figure C. 20 Pullout force-displacement curve for Cu=14 at normal stress of 69 kPa**

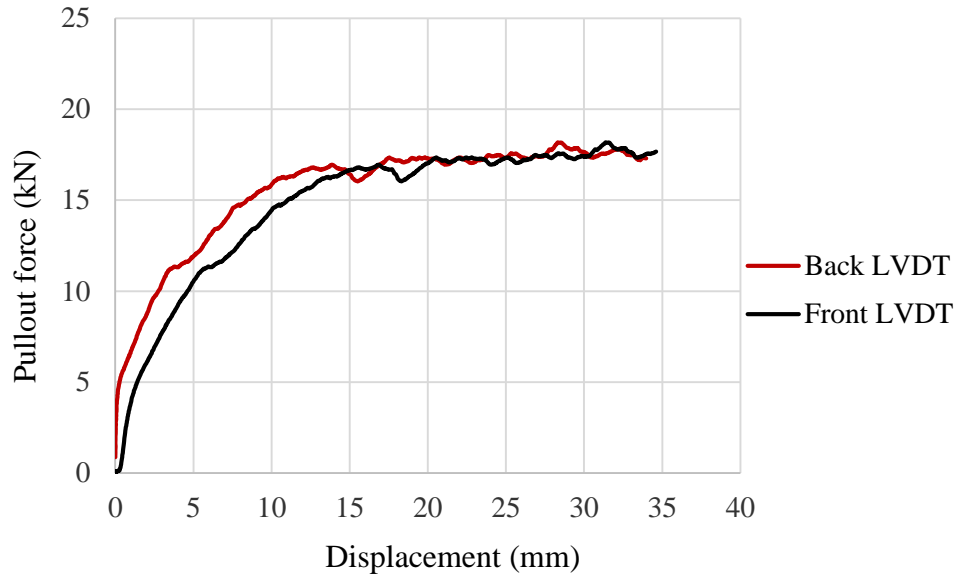


**Figure C. 21 Pullout force-displacement curve for Cu=14 at normal stress of 103 kPa**

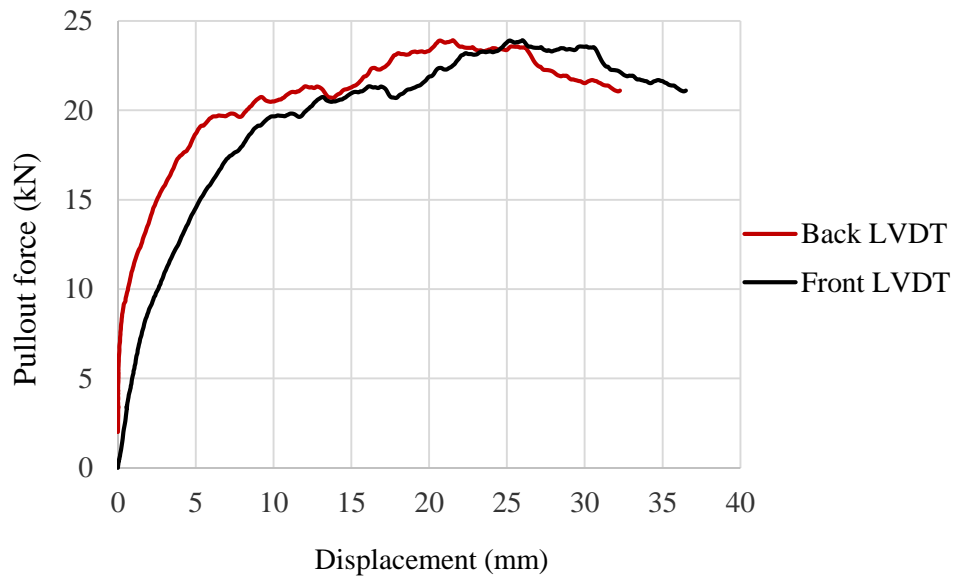


**Figure C. 22 Pullout force-displacement curve for Cu=14 at normal stress of 138 kPa**